



People`s Democratic Republic of Algeria  
Ministry of Higher Education and Scientific Research  
University of Echahid Hamma Lakhdar - El Oued



Faculty of Technology  
Department of Mechanical Engineering

Dissertation

ACADEMIC MASTER

Domain: Science and Technology

Division: Mechanical Engineering

Specialty: Electromechanical

**Presented by:**

1. Ad Houdaifa
2. Ferhat Seradj Eddine
3. Soualah Bedadi Bachir

**Entitled:**

**Comparative Study of MPPT Techniques for Photovoltaic System**

Dissertation Submitted in Partial Fulfillment of the Requirements for the Master Electromechanical

Degree in : .....

Publicly defended in: 29/05/2025

Board of Examiners:

**Dr. Miloudi Khaled**

**Dr. Largot soulef**

**Dr. Bebboukha Ali**

**Dr. Chabani Mohammed Saci**

**Chairman**

**Supervisor**

**Co-Supervisor**

**Examiner**

**Academic Year: 2024/2025**





# Dedication

To my dear parents

who have always been a source of strength and support, and who never hesitated to offer me advice and guidance. I extend my deepest gratitude for the love and care you have given me, as you were the foundation upon which this success was built.

To my esteemed teachers

who generously shared their knowledge and experience, and continuously guided me in the right direction. Thank you for your unwavering support, belief in my abilities, and motivating me to strive for excellence.

To my dear friends

who stood by my side at every step, never hesitating to offer help and encouragement. Thank you for always being there, as your support was a driving force in overcoming challenges and achieving this accomplishment.

And finally, to myself

for being patient and persistent, and for not giving up despite the hardships. I dedicate this success to myself and take pride in what I have achieved.

# Acknowledgment

First of all, I thank God—ALLAH—almighty for giving me the courage and patience throughout all these years of study.

I would like to express my sincere gratitude and thanks to **Dr. Largot Soulef**, Doctor at the Echahid Hamma Lakhdar University of El Oued, for having directed this work.

My sincere thanks to the members of the jury for the honor they have bestowed upon me by participating in the judging of this thesis.

We would like to sincerely thank everyone who helped us develop and complete this thesis, as well as all those who have helped us, directly or indirectly, to complete this work.

Finally, I would like to thank **Dr . Bebboukha Ali**. No matter how long I talk about him, words will never do him justice..

## **Abstract**

Solar radiation constitutes the principal energy source for photovoltaic (PV) systems, which convert sunlight directly into electrical energy via the photovoltaic effect. This study investigates the fundamental principles of PV systems and solar energy generation, with particular attention to spatial and seasonal variability. DC-DC converters are integral to these systems, facilitating efficient voltage level conversion to ensure stable power output. To enhance the efficiency of PV systems, Maximum Power Point Tracking (MPPT) algorithms are employed to continuously adjust the operating point, thereby extracting the maximum possible power from solar panels under fluctuating environmental conditions. This research evaluates and compares three commonly utilized MPPT algorithms—Perturb and Observe (P&O), Incremental Conductance (INC), and Artificial Neural Network (ANN).

The P&O algorithm operates through periodic perturbation and observation, INC is based on incremental conductance techniques, and ANN utilizes artificial intelligence to achieve accurate maximum power point tracking. This comprehensive analysis delineates the advantages, limitations, and applicability of each algorithm, offering insights for improving the overall efficiency and energy output of PV systems.

**Keywords:**

Maximum Power Point Tracking (MPPT), Perturb and Observe (P&O), Photovoltaic systems (PV), Incremental Conductance (INC), Solar energy Artificial Neural Networks (ANN).

## الملخص :

تُعد الإشعاعات الشمسية المصدر الرئيسي للطاقة في أنظمة الخلايا الكهروضوئية (PV)، حيث يتم تحويل ضوء الشمس مباشرة إلى طاقة كهربائية عبر التأثير الكهروضوئي. تتناول هذه الدراسة المفاهيم الأساسية لأنظمة الطاقة الكهروضوئية وتوليد الطاقة الشمسية، مع الأخذ في الاعتبار التغيرات الناتجة عن الموقع الجغرافي والتقلبات الموسمية. تلعب محولات التيار المستمر إلى التيار المستمر (DC-DC) دورًا حيويًا في هذه الأنظمة من خلال تحويل مستويات الجهد بكفاءة لضمان استقرار الإمداد بالطاقة. ولتحقيق أقصى كفاءة لأنظمة الطاقة الكهروضوئية، تُستخدم خوارزميات تتبع نقطة القدرة القصوى (MPPT) لضبط نقطة التشغيل باستمرار، بهدف استخلاص أكبر قدر ممكن من الطاقة من الألواح الشمسية في ظل الظروف المتغيرة. تقيّم هذه الدراسة ثلاث خوارزميات شائعة الاستخدام في تتبع نقطة القدرة القصوى، وهي: خوارزمية الاضطراب والملاحظة (P&O)، وخوارزمية التوصيل التزايدية (INC)، والشبكة العصبية الاصطناعية (ANN). تعتمد خوارزمية P&O على إدخال اضطرابات ومراقبة التغيرات الناتجة عنها، بينما تستخدم خوارزمية INC التوصيل التزايدية، في حين تعتمد خوارزمية ANN على تقنيات الذكاء الاصطناعي لتحقيق تتبع دقيق لنقطة القدرة القصوى. تقدم هذه الدراسة تحليلاً شاملاً يوضح مزايا وعيوب وإمكانيات كل خوارزمية، مما يوفر رؤى قيمة لتحسين الأداء العام وكفاءة توليد الطاقة في أنظمة الخلايا الكهروضوئية.

## الكلمات المفتاحية:

تتبع أقصى نقطة للقدرة (MPPT)، خوارزمية الاضطراب والمراقبة (P&O)، أنظمة الخلايا الضوئية (PV)، خوارزمية التوصيل التفاضلي (INC)، الطاقة الشمسية، الشبكات العصبية الاصطناعية (ANN).

**Contents**

<b>Headlines</b>	<b>Pages</b>
Dedication	I
Acknowledgments	II
Abstract	III
Contents	V
List of Figures	VIII
List of Tables	XI
List of Acronyms and Abbreviations	XII
General Introduction	1
<b>Chapter I : Solar Radiation and Photovoltaic Energy</b>	
I.1. Introduction	4
I.2. Solar Radiation	4
I.2.1. Radiation Spectrum	5
I.3. Conversion of Solar Radiation by PV Effect	6
I.4. Photovoltaic Generator	7
I.4.1. Photovoltaic Cell	9
I.4.2. Modelling of a PV Cell	10
I.4.3. Types of Photovoltaic Cells	12
I.5. The Impact of Temperature on Solar Panel	14
I.6. Advantages and Disadvantages of PV Energy	15
I.6.1. Advantages	15
I.6.2. Disadvantages	16
I.7 Conclusion	17
<b>Chapter II : DC-DC Converter</b>	
II.1. Introduction	18

## Contents

---

II.2. DC-DC Converters	18
II.3. Applications of DC-DC Converter	19
II.4. Types of DC-DC converters	21
II.4.1. Buck Converter	21
II.4.2. Boost Converter	26
II.4.3. Buck-Boost Converter	31
II.5. Comparison of Converter Types	35
II.6. Efficiency of Static Converters	35
II.7. Conclusion	36
<b>ChapterIII:Maximum Power Point Tracking</b>	
III.1. Introduction	38
III.2. Maximum Power Point Tracking	38
III.3. Working principle of MPPT	39
III.4. Classification of MPPT Control	41
III.4.1. Classification of MPPT Controllers Based on Input Parameters	41
III.4.2. Classification of MPPT Controllers According to the Type of Search	42
III.5. Different MPPT Commands Synthesis	43
III.5.1. First MPPT Commands Types	43
III.5.2. Efficient MPPT Commands Algorithms	44
III.5.2.1. Algorithm Perturb and Observe (P&O)	44
III.5.2.2. Algorithm Hill Climbing	48
III.5.2.3. Algorithm Incremental conductance (INC)	49
III.5.2.4. Artificial Neural Networks (ANN)	50
III.5.2.4.1. Application of Artificial Neural Networks in MPPT	51
III.5.2.4.2. Implementation of ANN in MATLAB/SIMULINK	51
III.6. Conclusion	57

## Contents

---

<b>ChapterIV: System Results</b>	
IV.1. Introduction	58
IV.2. Parameters of System Simulation	58
IV.3. Simulation Results	59
IV.3.1. Constant Irradiance (1000 W/m <sup>2</sup> )	59
IV.3.2. Variable Irradiances (1000, 800, 600, 1000W/m <sup>2</sup> )	66
IV.4. Comparison of efficiency between algorithms (P&O, INC, ANN)	70
IV.4.1. Constant Irradiance (1000 W/m <sup>2</sup> )	70
IV.4.2. Variable Irradiances (1000, 800, 600, 1000W/m <sup>2</sup> )	71
IV.5 Conclusion	72
General Conclusion	73
References	75

**List of Figures**

<b>Figures</b>	<b>Pages</b>
<b>Chapter I : Solar Radiation and Photovoltaic Energy</b>	
Figure (I.1): Representation of Solar Radiation	5
Figure (I.2): Solar Radiation Spectrum	5
Figure (I.3): Representation of Solar Radiation Spectrum	6
Figure (I.4): Solar Radiation Conversion by PV Effect	7
Figure (I.5): Adaptation Stage between a GPV and a load	8
Figure (I.6): Typical characteristics of a PV Generator	9
Figure (I.7): Working principle of Photovoltaic Cell	10
Figure (I.8): Equivalent Circuit of a PV Cell	11
Figure (I.9): Monocrystalline Cells	12
Figure (I.10): Polycrystalline Cells	12
Figure (I.11): Thin-Film Cells	13
Figure (I.12): Multijunction Cells	14
<b>Chapter II: DC-DC Converter</b>	
Figure (II.1): DC-DC Converters	19
Figure (II.2): Applications Of DC/DC Converters	20
Figure (II.3): The Circuit Representation of Buck Converter	22
Figure (II.4): Buck Converter When S1 is Closed	22
Figure (II.5): Buck Converter When S2 is Closed	24
Figure (II.6): Waveform Representation	26
Figure (II.7): Elementary Circuit of Boost Converter	27
Figure (II.8): The Chopper CH Is in On State	27
Figure (II.9): The Chopper CH Is in Off State	28
Figure (II.10): Waveform Representation	29

## List of Figures and Tables

Figure (II.11): The Circuit Representation of Buck-Boost Converter	31
Figure (II.12): The Equivalent Circuit of Mode I	32
Figure (II.13): The Equivalent Circuit of Mode II	33
<b>Chapter III: Maximum Power Point Tracking</b>	
Figure (III.1): Block Diagram of The PV System	40
Figure (III.2): Search and Recovery Of MPP	41
Figure (III.3): Bloc Diagram of a Digital MPPT Command	44
Figure (III.4): Ppv VS Vpv Characteristic of a Solar Panel	45
Figure III.5): Divergence of the P&O Command Due to Radiation Variations	46
Figure (III.6): Algorithm of the P&O Type of Command	46
Figure (III.7): State Flowchart of Hill Climbing MPPT Technique	48
Figure (III.8): Flowchart for The Incremental Conductance Algorithm	49
Figure (III.9): Functioning of Artificial Neural Networks	50
Figure (III.10): Setting Up the Neural Network Fitting Tool	52
Figure (III.11): Neural Network Structure	52
Figure (III.12): Import Data	53
Figure (III.13): Validation and Test Data	54
Figure (III.14): Network Architecture	54
Figure (III.15): Network Training	55
Figure (III.16): Train Network	56
<b>Chapter IV: System Results</b>	
Figure (IV.1): Characteristics of Panel	58
Constant Irradiance (1000 W/m <sup>2</sup> )	
P&O Algorithm	
Figure (IV.2): Schema of System Simulation With P&O	59
Figure (IV.3): Duty Cycle Simulation Result	59
Figure (IV.4): Power Simulation Result	60
Figure (IV.5): Voltage Simulation Result	60

## List of Figures and Tables

Figure (IV.6): Current Simulation Result	61
Incremental Conductance	
Figure (IV.7) : Schema of System Simulation With INC	61
Figure (IV.8): Power Simulation Result	62
Figure (IV.9): Voltage Simulation Result	62
Figure (IV.10): Current Simulation Result	63
Artificial Neural Network (ANN)	
Figure (IV11) : Schema of System Simulation With ANN	63
Figure (IV.12): Duty Cycle Simulation Result	64
Figure (IV.13): Power Simulation Result	64
Figure (IV.14): Voltage Simulation Result	65
Figure (IV.15): Current Simulation Result	65
Variable Irradiances (1000, 800, 600, 1000 W/m <sup>2</sup> )	
P&O Algorithm	
Figure (IV.16): Power Simulation Result	66
Figure (IV.17): Voltage Simulation Result	66
Figure (IV.18): Current Simulation Result	67
Incremental Conductance	
Figure (IV.19): Power Simulation Result	67
Figure (IV.20): Voltage Simulation Result	68
Figure (IV.21): Current Simulation Result	68
Artificial Neural Network (ANN)	
Figure (IV.22): Power Simulation Result	69
Figure (IV.23): Voltage Simulation Result	69
Figure (IV.24): Current Simulation Result	70
Comparison of efficiency between algorithms (P&O, INC, ANN)	
Constant Irradiance (1000 W/m <sup>2</sup> )	
Figure (IV.25): Chart of Efficiency	71

## List of Figures and Tables

---

Variable Irradiances (1000, 800, 600, 1000 W/m <sup>2</sup> )	
Figure (IV.26): Chart of Efficiency	72

## List of Tables

<b>Tables</b>	<b>Pages</b>
Table (II.1): Comparison of Converter Types	35
Table (II.2): Efficiency of Static Converters	35
Table (IV.1): Parameters of Boost Converter	58
Constant Irradiance (1000 W/m <sup>2</sup> )	
Table (IV.2): Table of Efficiency	70
Variable Irradiances (1000, 800, 600, 1000W/m <sup>2</sup> )	
Table (IV.3): Table of Efficiency	71

**List of Acronyms and Abbreviations**

<b>List of Abbreviations</b>	
<b>MPP</b>	Maximum power point
<b>MPPT</b>	Maximum power point tracking
<b>DC-DC</b>	Continuous-continuous converter
<b>P&amp;O</b>	Perturb and observe
<b>INC</b>	Incremental Conductance
<b>ANN</b>	Artificial neural network
<b>PV</b>	Photovoltaic
<b>MOSFET</b>	Metal Oxide Semiconductor Field Effect Transistor
<b>LED</b>	Light Emitting Diode
<b>PWM</b>	Pulse Width Modulation
<b>KVL</b>	Kirchhoff's Voltage Law

<b>List of Acronyms</b>	
<b>L</b>	Inductance (mH)
<b>Rs</b>	Series resistance( $\Omega$ )
<b>Rsh</b>	Shunt resistance ( $\Omega$ )
<b>R<sub>opt</sub></b>	The optimal value of the load resistance( $\Omega$ )
<b>R<sub>c</sub></b>	The load resistance( $\Omega$ )
<b><math>\eta</math></b>	The energy efficiency of the solar cell (%)
<b>G</b>	The conductance value( $1000 \text{ W/m}^2$ )
<b>V<sub>oc</sub></b>	Open circuit voltage (V)
<b>I<sub>oc</sub></b>	Open circuit current(A)
<b>I<sub>sc</sub></b>	The short circuit current (A)
<b>P<math>\gamma</math></b>	The incident light power on the surface of the cell
<b>D</b>	The duty cycle

## List of Acronyms and Abbreviations

---

<b><math>W_{on}</math></b>	The energy input provided by the source to the inductor when CH is on
<b><math>W_{off}</math></b>	The energy that the inductor releases to the load when CH is off
<b>T</b>	The total time period (S)
<b>CH</b>	The chopper
<b><math>V_L</math></b>	The voltage across the inductor (V)
<b><math>f_{switching}</math></b>	The switching frequency (kHz)
<b>Pmax</b>	The value of the maximum real power (W)

**General**

**Introduction**

### General Introduction

The global population is experiencing a rapid increase, accompanied by a corresponding rise in energy consumption. As a result, there is a growing demand for electricity generation, which in turn necessitates the use of additional resources. To date, fossil fuels have served as the primary energy source; however, these are finite and non-renewable. Consequently, the exploration and adoption of sustainable and inexhaustible energy alternatives have become imperative.

Among renewable energy sources, solar energy is regarded as one of the most sophisticated and promising options. It operates silently, integrates seamlessly with architectural structures (such as facades and rooftops), and, due to the absence of moving mechanical components, requires minimal maintenance while offering long-term reliability. These characteristics have established solar energy as a standard solution for space applications and remote locations. Moreover, advancements in technology have led to a reduction in the cost of solar panels and improvements in their efficiency, thereby making solar energy increasingly viable for small- to medium-scale energy consumption.

This study focuses on enhancing the efficiency and performance of photovoltaic (PV) solar energy systems through the implementation of a Maximum Power Point Tracking (MPPT) controller under varying environmental conditions, including solar irradiance and temperature. Specifically, the research involves the simulation of a photovoltaic energy system comprising a solar panel and a DC/DC boost converter[1]

# **Chapter I**

## **Solar Radation and Phptovoltaic Energy**

**I.1. Introduction :**

Solar radiation is the energy emitted by the sun, which can be harnessed to generate electricity. Photovoltaic (PV) energy uses solar cells to convert this radiation into electrical power through the photoelectric effect. PV technology offers a clean, renewable solution to reduce dependence on fossil fuels..

In this chapter, we will discuss general information about solar energy. We will describe the basic concepts of photovoltaic systems and electricity production through the photovoltaic effect. We will explain how solar energy varies depending on location and season. [2]

**I.2. Solar Radiation:**

Solar energy refers to the energy harnessed from the Sun's radiation. This renewable energy source is captured using photovoltaic cells, which convert sunlight directly into electricity, or through solar thermal systems that generate heat for various applications. The conversion of solar radiation into electricity is accurately modeled by the photovoltaic effect, where semiconductor materials generate an electric current when exposed to light. The efficiency of solar panels depends on factors such as sunlight intensity, angle of incidence, and temperature. Most commercial solar cells operate with an efficiency range of 15% to 22%. Upon reaching the Earth's surface, solar energy undergoes several atmospheric interactions, including absorption and scattering by gases, dust, and clouds. Notably, the ozone layer absorbs a significant portion of harmful ultraviolet radiation, allowing primarily visible and infrared light to reach the ground for energy generation [3] .



Figure (1.1): Representation of Solar Radiation

**I.2.1. Radiation Spectrum:**

The radiation spectrum encompasses the entire range of electromagnetic waves emitted by various sources, including the Sun. It consists of different types of radiation, ranging from high-energy gamma rays to low-energy radio waves. Each type of radiation is characterized by its wavelength and frequency, with shorter wavelengths corresponding to higher energy levels [4].

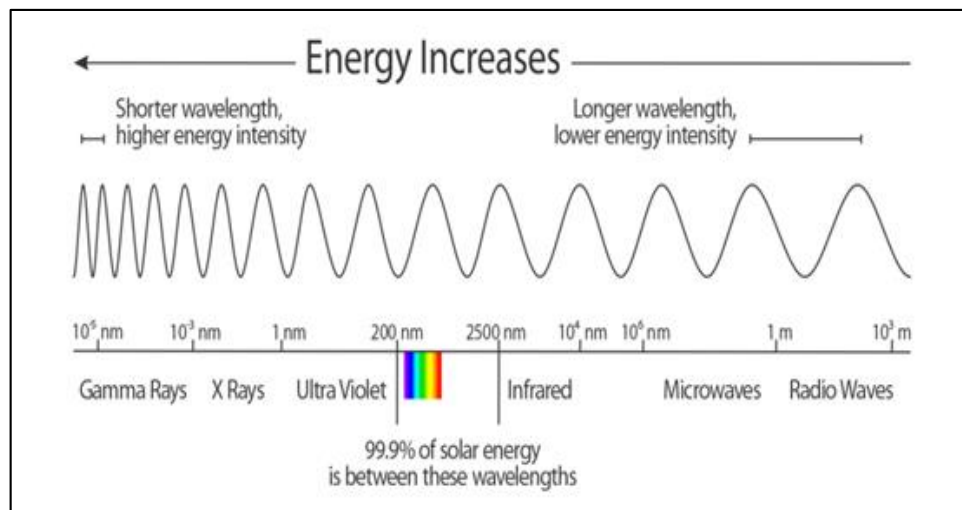


Figure (1.2): Solar Radiation Spectrum

Solar radiation, which powers life on Earth, mainly falls within the ultraviolet, visible, and infrared regions of the spectrum. While the Sun emits energy across a broad range, approximately 99% of its radiation is concentrated between 200 and 2500 nanometers.

The Earth’s atmosphere plays a crucial role in filtering harmful radiation, such as most ultraviolet rays, while allowing visible and infrared light to pass through. Only a fraction of the Sun’s radiation reaches the Earth’s surface, as atmospheric gases, water vapor, and dust absorb or scatter some of the energy [2] .

Figure (I.3) illustrates The Solar Radiation spectrum .The composition of solar energy that reaches the surface is approximately 5% ultraviolet, 42% visible light, and 53% infrared radiation, making it essential for processes like photosynthesis and solar power generation.

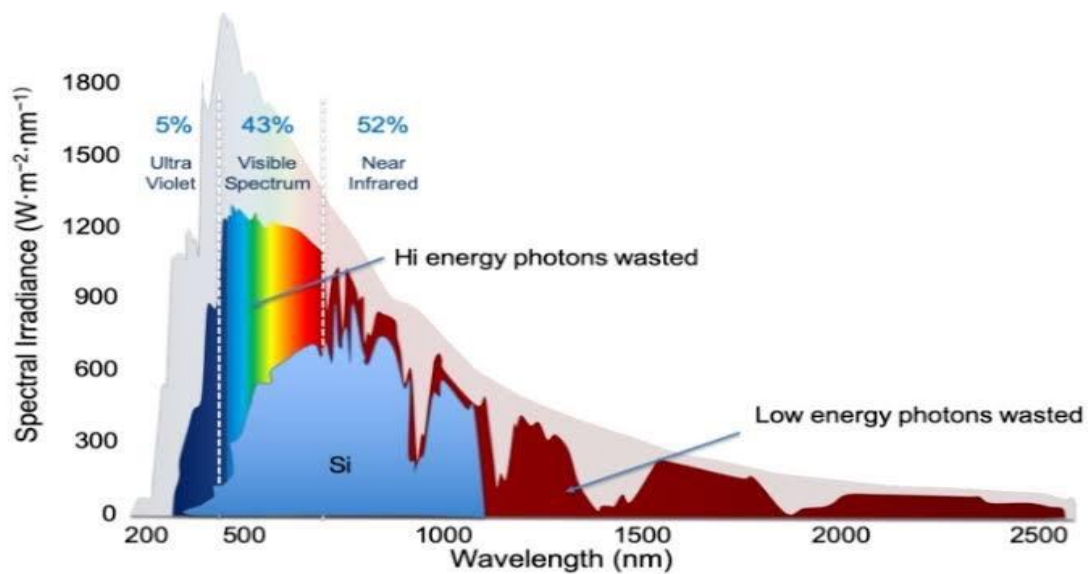


Figure (I.3): Representation of Solar Radiation Spectrum

**I.3. Conversion of Solar Radiation by PV Effect:**

Photovoltaic (PV) cells convert sunlight into electricity using the photovoltaic effect. These cells consist of two layers of silicon: a positively doped “P-layer” with boron atoms and a negatively doped “N-layer” with phosphorus atoms. This doping creates a potential difference between the layers. When sunlight strikes the semiconductor material, photons transfer their energy to electrons, freeing them from their atomic bonds. This process generates electron movement, creating an electric current. The generated electricity can then be used to power devices or stored in batteries for later use [1].

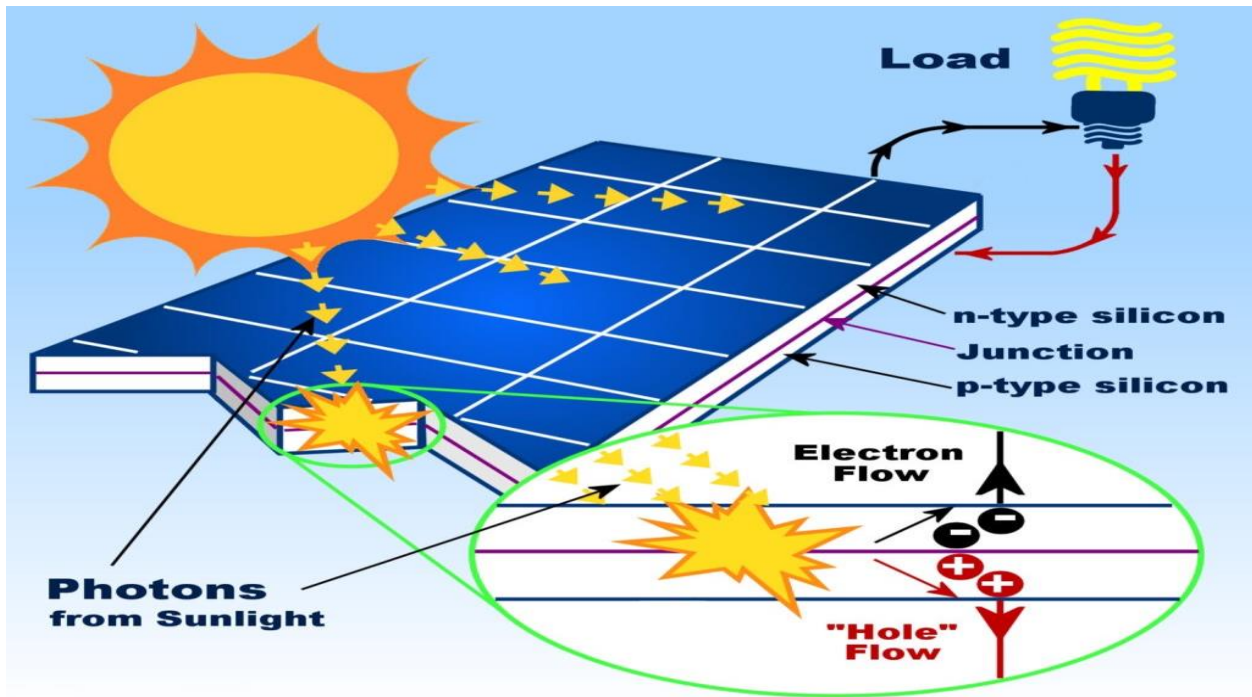


Figure (1.4): Solar Radiation Conversion by PV Effect

#### I.4. Photovoltaic Generator:

The GPV represents the part of conversion of the energy contained in the light of the sun into direct current electrical energy. This part is essentially composed of a set of VPs. Structured in series or parallel or hybrid (Mixed)[5]. To guarantee a significant lifespan of a photovoltaic installation intended to produce energy. Photovoltaic generators have non-linear current-voltage characteristics and have a maximum power point (MPP). This characteristic depends on the level of lighting and temperature. Therefore, the operating point of the PV generator can vary between these points. Corresponds to the extreme values of the short-circuit current and the no-load voltage. The module is composed of 54 monocrystalline cells connected in series ( $N_s=54$ )[6]. Remember that these parameters are given for reference conditions, i.e.  $G_{ref} = 1000$  W/m<sup>2</sup> and  $T_{ref} = 25^\circ\text{C}$

.In order to always extract the maximum power available at the terminals of the PV generator and transmit it to the load, a commonly used technique is to use an adaptation stage between the PV generator and the load, as shown in Figure

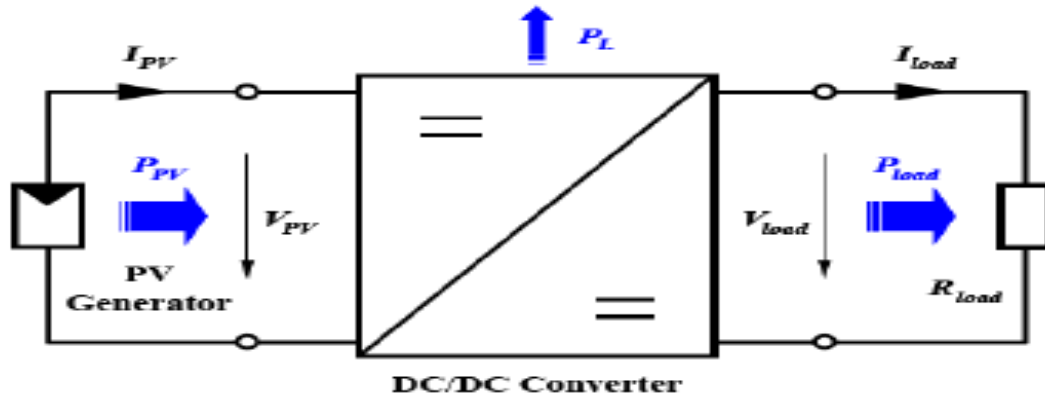


Figure (1.5): Adaptation stage between a GPV and a load

This stage acts as an interface between two elements by ensuring that an action Control, transmission of the maximum power supplied by the generator. The latter can allow the generator to provide its maximum power by specific command, denoted  $P_{max}$  ( $P_{max} = V_{opt} * I_{opt}$ ) where  $V_{opt}$  and  $I_{opt}$  respectively represent the voltage and for a given I-V curve, Optimal current for the photovoltaic generator, while ensuring that the voltage or current of the load corresponds to the characteristics of the latter. To keep photovoltaic generators operating at their optimum level as often as possible, the usual solution is to introduce static converters as a source-to-load adapter. The DC-DC converter operates the modules at the optimal power point independent of lighting and load[7].

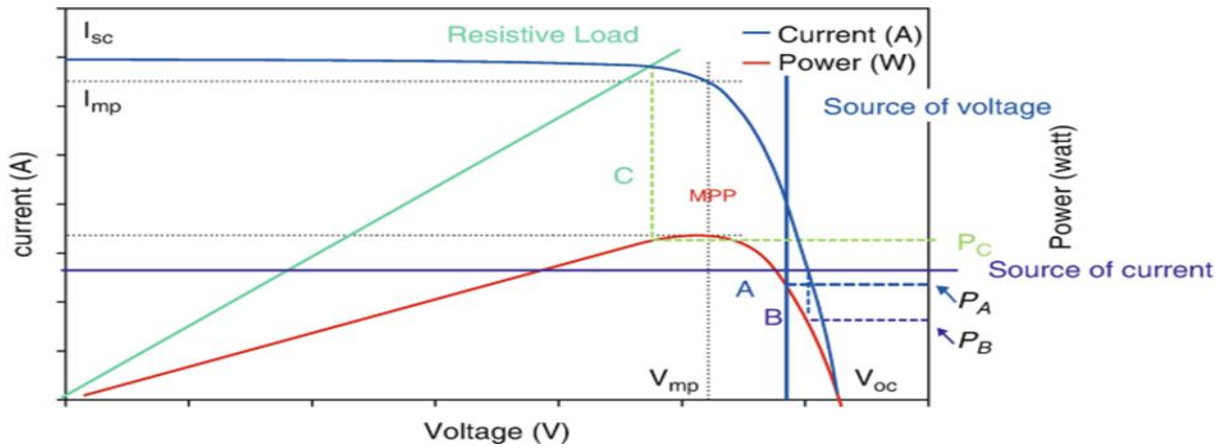


Figure (1.6): Typical Characteristics of a PV Generator

**I.4.1. Photovoltaic Cell:**

A photovoltaic cell is a specific type of PN junction diode that is intended to convert light energy into electrical power. These cells usually operate in a reverse bias environment. Photovoltaic cells and solar cells have different features, yet they work on similar principles. Photovoltaic cells are essential for turning incident light into electrical energy that can be used, and their ability to function in a reverse bias situation emphasizes how specifically engineered they are to maximize solar power.

It is interesting to note that despite the fact that these names may pertain to distinct facets of the technology, their close proximity to the process of turning sunlight into electrical power makes them often used interchangeably.

Photovoltaic cells are essential for turning incident light into electrical energy that can be used, and their ability to function in a reverse bias situation emphasizes how specifically engineered they are to maximize solar power [8].

It is interesting to note that despite the fact that these names may pertain to distinct facets of the technology, their close proximity to the process of turning sunlight into electrical power makes them often used interchangeably.

Working principle of Photovoltaic Cell is similar to that of a diode. In PV cell, when light whose energy ( $h\nu$ ) is greater than the band gap of the semiconductor used, the light gets trapped and used to produce current. In the absorption layer of the cell, photons from sunlight provide electrons energy, which causes the electrons to break free from their atomic connections and form electron-hole pairs. These charge carriers separate

more easily at the P-N junction due to the electric field there, which pushes holes toward the P-type region and electrons toward the N-type region[8].

.When an external circuit is linked, the space separation between the two sides generates a voltage potential that causes electrons and holes to flow, producing an electric current

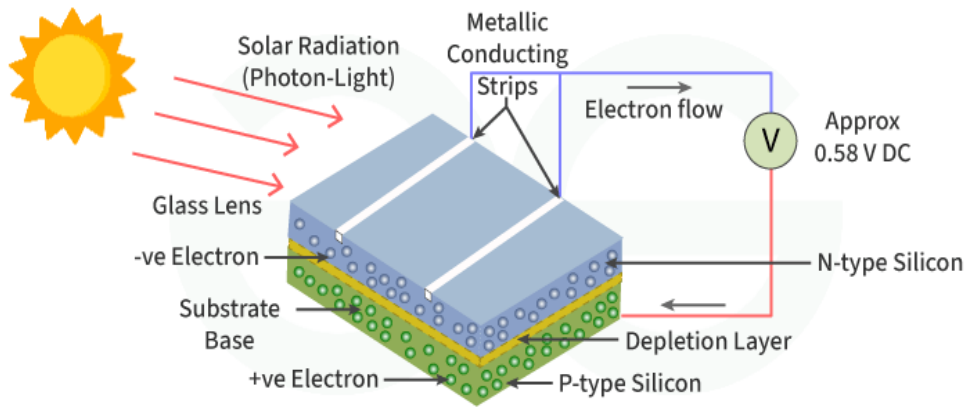


**Figure (1.7):** Working principle of Photovoltaic Cell

#### 1.4.2. Modelling of a PV Cell:

A photovoltaic cell is a non-linear energy source. The module's output current and voltage depend on the solar irradiance  $S$  and the temperature  $T$ . For this reason, predicting the performance of a photovoltaic cell requires the development of a mathematical model in order to study its behavior under different conditions. Weather (light, temperature). Many studies focus on the development of a mathematical model for simulating the current-voltage ( $I, V$ ) characteristics of photovoltaic cells. In this section, we will present some models of photovoltaic cells in the existing literature. Next, we explain the modifications made to the battery model to describe the current-voltage relationship of a photovoltaic generator. The equivalent circuit of a photovoltaic (PV) cell represents the electrical behavior of the cell in terms of passive circuit elements such as resistors, diodes, and current sources. This simplified model helps in analyzing the performance of the PV cell under different operating conditions[9].

The equivalent circuit of a PV cell typically consists of the following components  
 Photovoltaic Current Source ( $I_{ph}$ ): This represents the current generated by the PV cell

when exposed to light. It is proportional to the intensity of incident light and the efficiency of the cell.

**Diode :** The diode represents the behavior of the p-n junction within the PV cell. It accounts for the voltage drop across the junction and the recombination losses within the cell. The diode equation is often used to model this behavior [10].

**Series Resistance ( $R_s$ ):** This represents the internal resistance of the PV cell, including the resistance of the semiconductor material and the metal contacts. It causes a voltage drop across the cell when current flows through it.

**Shunt Resistance ( $R_{sh}$ ):** This represents any parallel paths for current flow within the cell such as surface leakage or defects in the semiconductor material. It affects the overall current-voltage characteristics of the cell.

**Load Resistance ( $R_L$ ):** This represents the external load connected to the PV cell, such as a battery or an electrical device. It affects the operating point of the cell and determines the maximum power output [11].

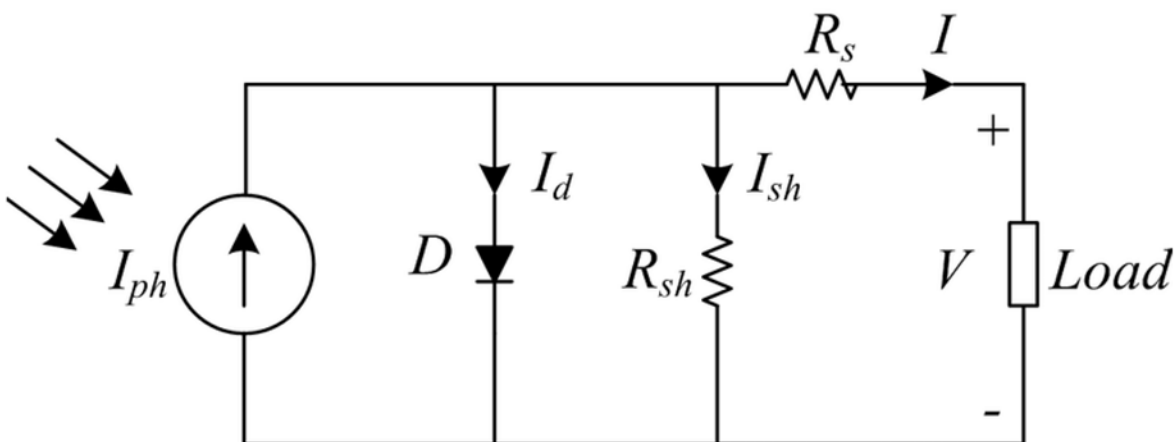


Figure (I.8) : Equivalent Circuit of a PV Cell

### 1.4.3. Types of Photovoltaic Cells :

There are several types of photovoltaic cells, each employing different materials and

technologies to convert sunlight into electricity. The main types of photovoltaic cells include:

### 1. Monocrystalline Cells:

Monocrystalline cells are made from a single crystal structure, resulting in a high efficiency of solar energy conversion. These cells are known for their sleek appearance and high power output per square foot [12].



Figure (1.9):: Monocrystalline Cells

### 2. Polycrystalline Cells:

Polycrystalline cells are made from multiple crystal structures. While they are less efficient than monocrystalline cells, they are more cost-effective to produce.

Polycrystalline solar panels often have a blue tint

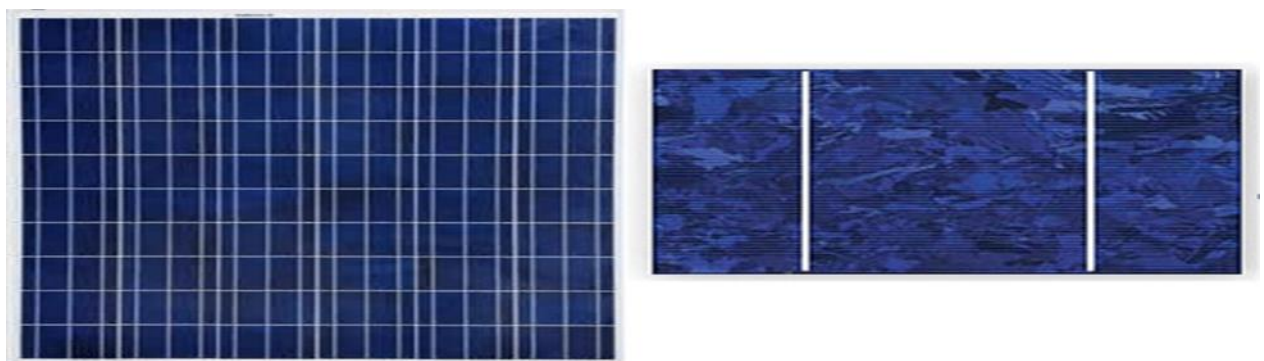
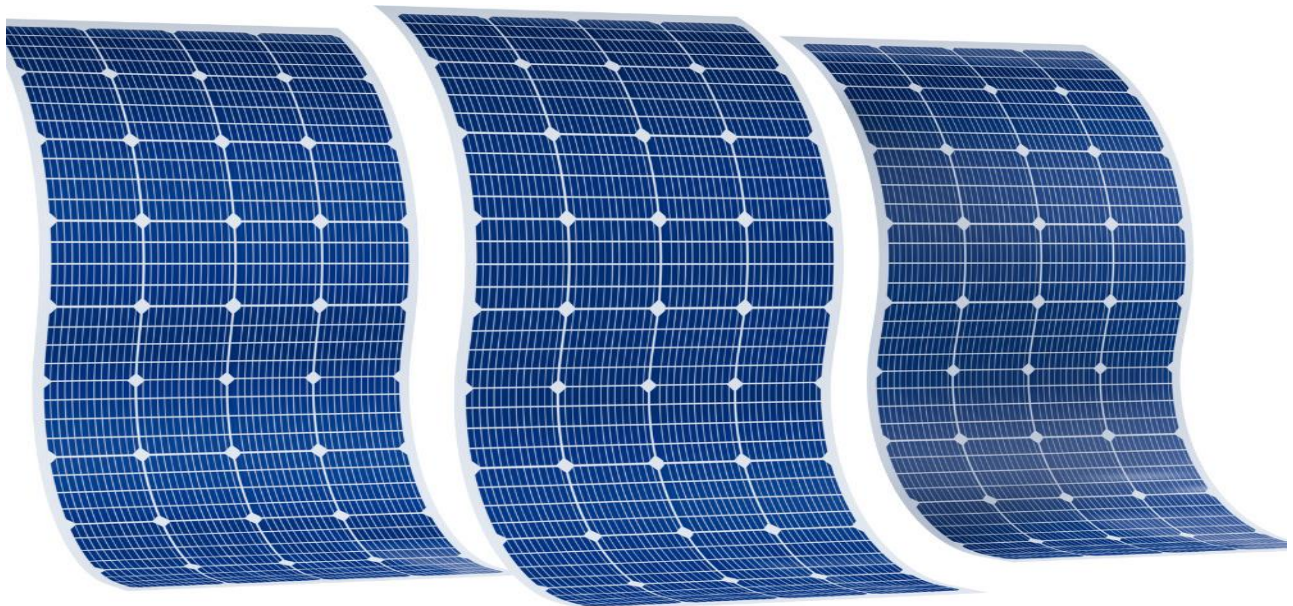


Figure (1.10): Polycrystalline Cells

### 3. Thin-Film Cells:

Thin-film solar cells use layers of semiconductor materials that are only a few micrometers thick. Common materials include amorphous silicon (a-Si), cadmium telluride (CdTe), and copper indium gallium selenide (CIGS). Thin-film cells are lightweight, flexible, and cost-effective but generally have lower efficiency



**Figure(I.11) :**Thin-Film Cells

### 4. Multijunction Cells:

Multijunction solar cells consist of multiple layers of semiconductor materials stacked on top of each other. Each layer is designed to absorb a specific range of wavelengths of sunlight, increasing the overall efficiency. These cells are often used in concentrated photovoltaic systems[13].

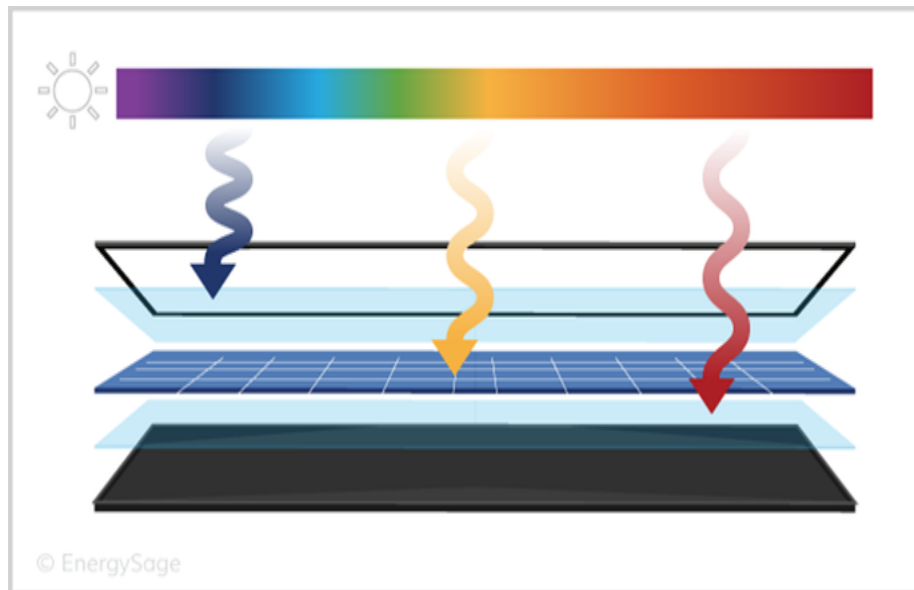


Figure (1.12): Multijunction Cells

### 1.5. The Impact of Temperature on Solar Panel:

Temperature has a significant impact on the performance of solar panels. Here's how:

- **Reduction in Efficiency:** The efficiency of solar panels decreases as temperature increases. This reduction occurs because solar cells, typically made from silicon, experience increased electrical resistance and reduced voltage output in high temperatures.
- **Voltage Decrease:** The voltage output of solar panels decreases as temperature increases, directly impacting their efficiency and power generation. This occurs because high temperatures increase the energy of electrons in the semiconductor material, reducing the potential difference (voltage) between the positive and negative terminals of the panel [14].
- **Power Output Reduction:** When the temperature of a solar panel increases, its power output decreases due to a drop in voltage. While current (amperage) may remain stable or slightly increase, the significant reduction in voltage leads to lower overall power generation.
- **Thermal Degradation:** Thermal degradation refers to the long-term reduction in a solar panel's performance due to prolonged exposure to high temperatures. Over time, excessive heat can cause material wear, efficiency loss, and structural damage, reducing the panel's overall lifespan and energy output.

- **Operating Temperature Range:** Solar panels are designed to function across a wide range of temperatures, but their efficiency and longevity can be affected by extreme heat or cold. The operating temperature range refers to the minimum and maximum temperatures at which a solar panel can function effectively without sustaining damage

Overall, while solar panels still generate electricity on hot days, their efficiency decreases as temperatures rise, impacting their overall performance and output.

## **1.6. Advantages and Disadvantages of PV Energy:**

### **1.6.1 Advantages:**

**1. Renewable and Sustainable:** PV energy is derived from the sun, which is an abundant and inexhaustible source of energy. Unlike fossil fuels, which deplete over time, sunlight is available daily and does not run out. As long as the sun exists, solar energy can be harnessed to generate electricity [15].

**2. Environmentally Friendly:** PV energy does not produce greenhouse gases, carbon emissions, or air pollutants during operation. Unlike coal and natural gas power plants, solar panels do not contribute to air pollution, acid rain, or global warming. This makes PV energy a clean and sustainable alternative to conventional power sources.

**3. Low Operating Costs:** Once installed, solar panels require minimal maintenance and have low operational costs. They do not have moving parts that wear out quickly, reducing the need for frequent repairs. Periodic cleaning and occasional inverter replacements are usually the only maintenance requirements.

**4. Energy Independence:** PV energy allows individuals, businesses, and even countries to reduce dependence on fossil fuels and imported energy. By generating their own electricity, homeowners and businesses can lower electricity bills and avoid energy price fluctuations caused by fuel shortages or geopolitical issues.

**5. Scalability and Versatility:** PV systems can be installed on a small or large scale, making them suitable for various applications. They can be used for residential rooftops, commercial buildings, industrial plants, and large solar farms. Additionally,

they can be installed in remote locations where traditional electricity grids are unavailable, providing power to rural and off-grid areas.

**6. Job Creation and Economic Growth:** The PV industry creates jobs in manufacturing, installation, maintenance, and research. As the demand for solar energy increases, more employment opportunities are generated, contributing to economic development and innovation in clean energy technologies.

**7. Silent Operation:** Unlike traditional power plants, solar panels operate silently because they do not have moving mechanical parts. This makes PV energy ideal for urban and residential areas where noise pollution is a concern.

### **I.6.2. Disadvantages:**

**1. High Initial Costs:** The upfront cost of purchasing and installing a solar PV system can be high. Expenses include solar panels, inverters, batteries (for storage), and installation labor. Although prices have been decreasing over the years, the initial investment is still a barrier for many homeowners and businesses. However, government incentives and financing options can help offset these costs.

**2. Weather Dependence:** PV systems rely on sunlight, meaning their efficiency is directly affected by weather conditions. Cloudy days, rain, snow, and fog can reduce energy production. Solar panels also do not generate electricity at night, requiring either a backup power source (such as the grid) or energy storage systems (batteries) to provide power during non-sunny hours.

**3. Space Requirements:** Solar panels require a significant amount of space to generate large amounts of electricity. While rooftops can accommodate small-scale installations, large solar farms need vast land areas, which may not always be available, especially in urban environments.

**4. Energy Storage Challenges:** Since PV systems do not generate power at night, batteries or grid connections are needed to store or supply electricity when solar production is low. However, energy storage technologies (such as lithium-ion batteries) are expensive and can add to the overall cost of the system. Additionally, batteries have a limited lifespan and require periodic replacements.

**5. Efficiency Limitations:** The efficiency of solar panels typically ranges between 15% and 22%, meaning a large portion of sunlight is not converted into electricity. Various factors, such as temperature, dust, shading, and panel degradation, can further reduce efficiency. Researchers are working on improving efficiency, but current technologies still have limitations.

**6. Manufacturing and Environmental Impact:** Although PV energy is clean during operation, the manufacturing process of solar panels involves the use of energy and chemicals. Producing silicon-based panels requires mining, refining, and processing materials, which can generate carbon emissions and toxic waste if not managed properly. However, advancements in recycling and sustainable manufacturing are helping to reduce this impact.

**7. Grid Integration Issues:** In areas with high solar penetration, integrating PV energy into existing electrical grids can be challenging. The intermittent nature of solar power requires grid operators to balance supply and demand effectively. Without proper infrastructure, sudden surges or drops in solar power production can cause grid instability.

### **I.7. Conclusion:**

In conclusion, this chapter explored the fundamentals of solar radiation and photovoltaic energy conversion. It detailed how solar cells utilize the photovoltaic effect to convert sunlight into electricity. The modeling and characteristics of photovoltaic generators were examined, along with factors affecting their efficiency, such as temperature and load resistance. Various types of photovoltaic cells based on silicon crystal structure were introduced. Additionally, the chapter discussed the components of photovoltaic modules and outlined the main advantages and disadvantages of solar photovoltaic technology[6].

# **Chapter II**

## **DC-DC Converter**

**II.1. Introduction :**

DC-DC converters represent fundamental electronic circuits that serve a vital function within contemporary power management systems. Their principal role involves converting the voltage level of a direct current (DC) source from one magnitude to another, thereby facilitating stable and efficient power delivery to a wide range of electronic devices and systems. In scenarios where input voltage levels are subject to variation due to factors such as battery discharge over time or fluctuations in load conditions, DC-DC converters are employed to regulate and maintain a constant output voltage, ensuring reliable power supply to system components. A notable advantage of DC-DC converters lies in their high power conversion efficiency. Through the implementation of switching techniques, these converters significantly reduce power losses typically associated with resistive components, such as transformers or linear regulators, which often result in heat generation and energy dissipation. Consequently, their application contributes to enhanced overall efficiency and extended battery life in portable electronic devices. Furthermore, DC-DC converters provide flexibility in adjusting voltage levels, enabling efficient power distribution within electronic systems. They are also capable of offering galvanic isolation, thereby electrically separating the input and output grounds to mitigate the risk of ground loops and to protect sensitive components from voltage transients and electrical noise[16].

**II.2. DC-DC Converters:**

DC-DC converters are classified as static power electronic converters that operate using a direct current (DC) voltage source to generate a controllable DC output voltage across a load. These converters can be designed utilizing thyristor-based configurations for high-power applications, typically in the range of several hundred megawatts (MW), operating at a chopping frequency of a few kilohertz (kHz). Alternatively, for lower power applications—ranging from several hundred watts to approximately 100 kilowatts (kW)—DC-DC converters are commonly implemented using transistor-based structures, which enable higher chopping frequencies of up to 100 kHz. The symbol representing a DC-DC converter is illustrated in the following figure[17].

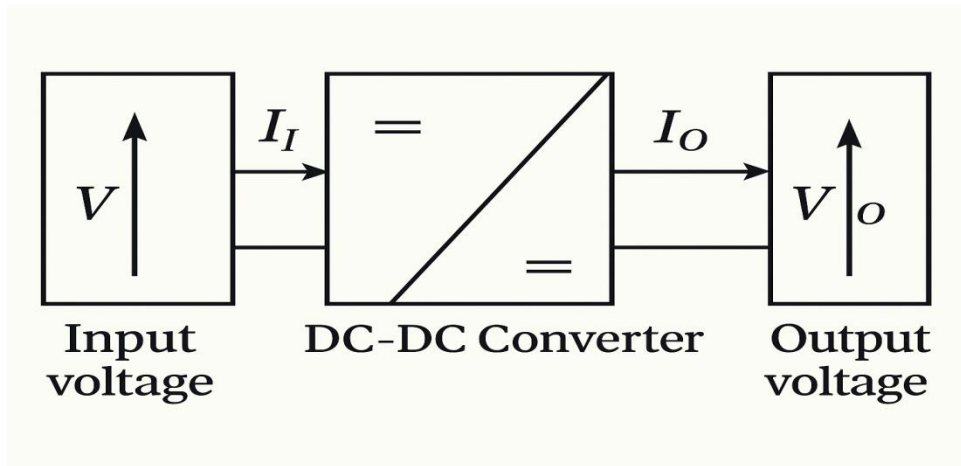


Figure (II.1): DC-DC Converters

### II.3. Applications of DC-DC Converter:

For several years, switch-mode power converters have been widely implemented in modern electronic systems across various sectors, including industrial, commercial, utility, and consumer markets. In low-power DC-DC conversion applications, the majority of contemporary power conversion processes are achieved using three fundamental types of power converters: buck, boost, and buck-boost converters. However, specific and specialized applications often necessitate the development of advanced configurations or modified variants of these conventional topologies to meet particular operational requirement[18].

Numerous DC-DC converter types are discussed in the literature; nevertheless, no single solution is universally applicable to all potential applications. Conversion techniques, in general, have found extensive use across various domains, including industry, research and development, and daily life.

DC-DC converters constitute a central focus of study within the field of power electronics and energy drives, given their widespread integration into numerous industrial applications. Some of these applications are illustrated in Figure (II.2). High voltage gain converters are employed in a variety of advanced applications, such as radar systems, DC distribution networks, data centers, and renewable energy integration[19].

This is particularly significant in the context of renewable energy applications, where high voltage gain DC-DC converters facilitate voltage boosting, making them

suitable for integration with distribution systems. DC distribution, in general, offers a range of advantages, including a reduced number of conversion units, lower cost, and enhanced power quality, thereby making it a preferred choice for many applications.

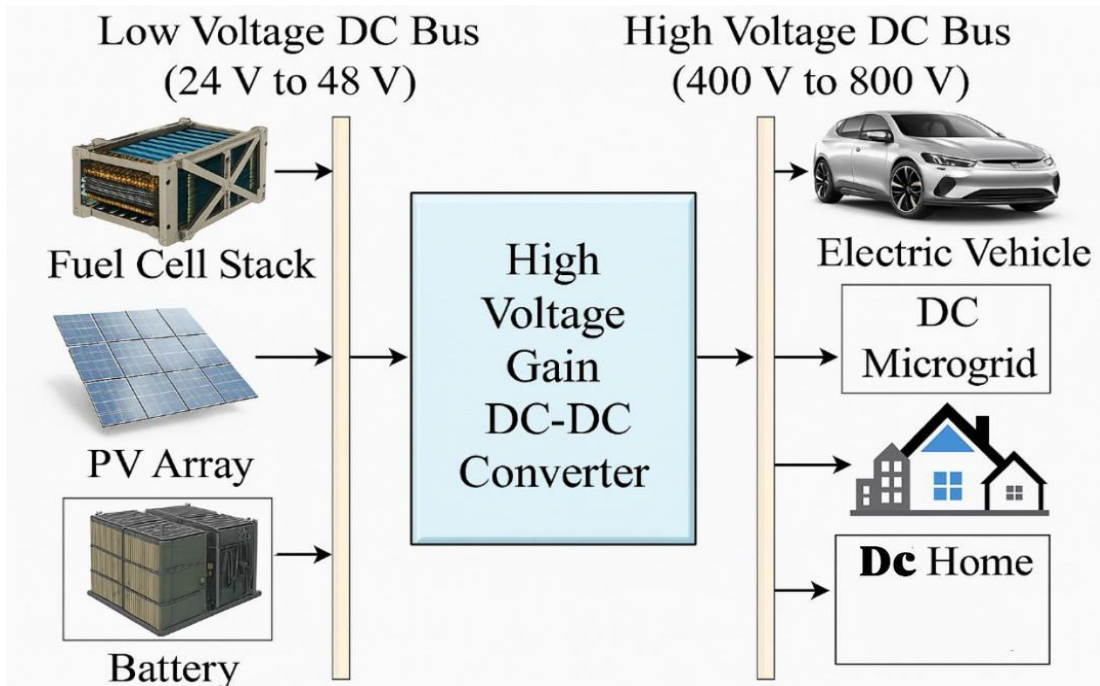


Figure (II.2): Applications of DC/DC Converters.

Applications of DC-DC Converters:

- **Renewable Energy Systems:**

In renewable energy applications, DC-DC converters must facilitate a continuous and smooth input current to minimize current ripple. Furthermore, these converters should be capable of integration with various power sources. Non-isolated, interleaved high-voltage gain converter topologies are commonly employed for interfacing renewable sources with micro grids [20].

- **Medical Equipment:**

Isolated DC-DC converters are vital in medical applications where electrical safety is paramount, as they effectively separate the output from potentially hazardous input voltages. Nonetheless, non-isolated converter types may also be used in applications such as power supplies for x-ray systems.

- **Automotive Systems:**

In vehicular systems, the principal DC-DC converter steps down the voltage

from the high-voltage onboard battery to supply lower DC voltages required for auxiliary loads such as lighting , windshield wipers, and window actuators [21] . This applies to both electric and hybrid electric vehicles . Electrical isolation is necessary when control systems must be separated from high-voltage domains. Buck-boost converters are used for voltage regulation, while charge-pump converters are employed for voltage inversion.

- **Smart Lighting Applications:**

Numerous lighting applications demand efficient LED backlight driver solutions featuring high performance , direct current regulation , overvoltage protection , pulse-width modulation (PWM) control , and simplified design. DC-DC converter types suitable for these functions include linear regulators, charge pumps, and conventional switching converters.

#### **II.4. Types of DC-DC converters:**

DC-DC converters are typically categorized into three fundamental types: Buck, Boost, and Buck-Boost converters.

##### **II.4.1 Buck Converter:**

The Buck Converter is a type of DC-DC converter designed specifically for step-down conversion of the applied DC input signal. Within this topology, a constant DC input voltage is transformed into a lower-magnitude DC output voltage. Consequently, the converter produces a DC signal with a reduced amplitude relative to the input. This converter is also commonly referred to as a Step-Down DC-DC Converter, Step-Down Chopper, or Buck Regulator.

#### **Operating Principle of Buck Converter**

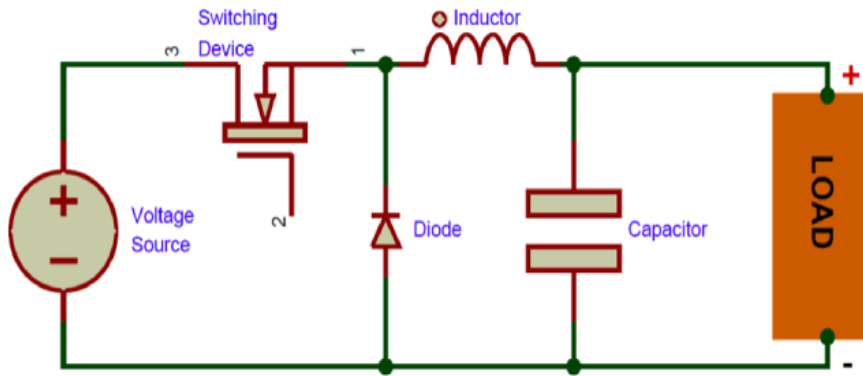


**Figure (II.3):** The Circuit Representation of Buck Converter

In the schematic presented above, the circuit comprises a power electronic solid-state device operating as a switch, along with a freewheeling diode that functions as an auxiliary switching component. These switching elements are integrated with a low-pass LC filter, which serves to attenuate current and voltage ripples, thereby ensuring the generation of a regulated DC output. A purely resistive load is connected across the circuit, representing the output load.

The circuit operates in two distinct modes. The first operational mode occurs when the power MOSFET (denoted as switch  $S_1$ ) is in the closed state. In this mode, the closure of switch  $S_1$  enables current to flow through the device, facilitating power transfer to the load

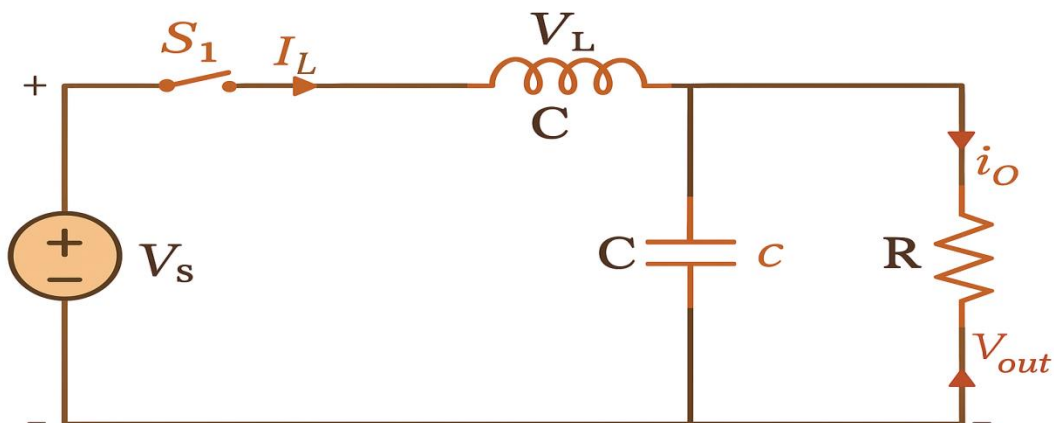


**Figure (II.4):** Buck Converter When  $S_1$  is Closed

initially, when a constant DC voltage is applied to the input terminals of the circuit and switch  $S_1$  is in the closed state, current begins to flow through the circuit, as

illustrated in the preceding diagram. As a consequence of this current flow, the inductor within the circuit stores energy in the form of a magnetic field. Additionally, the presence of a capacitor allows current to flow through it, leading to the storage of electrical charge. The voltage developed across the capacitor subsequently appears across the load.

In accordance with Lenz's Law, the energy stored in the inductor opposes the variation in current that originally induced it. This opposition results in the generation of an induced current and a reversal of polarity across the inductor

The total switching time period ( $T$ ) of the circuit operation comprises two intervals: the on-time ( $T_{on}$ ) and the off-time ( $T_{off}$ ).

$$T = T_{on} + T_{off} \quad (\text{II. 1})$$

The duty cycle is written as:

$$D = \frac{T_{on}}{T} \quad (\text{II. 2})$$

On applying KVL, in the above-given circuit

$$V_s = V_L + V_{out} \quad (\text{II. 3})$$

$$V_L = V_s - V_{out} \quad (\text{II. 4})$$

Also,

$$V_L = L \frac{di_L}{dt} = V_s - V_{out} \quad (\text{II. 5})$$

$$\frac{di_L}{dt} = \frac{V_s - V_{out}}{L} \quad (\text{II. 6})$$

When S1 is in closed condition then  $T_{on} = DT$  thus  $\Delta t = DT$ . Therefore, we can write

$$\frac{\Delta i_L}{\Delta t} = \frac{V_s - V_{out}}{L} \quad (\text{II. 7})$$

$$\frac{\Delta i_L}{DT} = \frac{V_s - V_{out}}{L} \quad (\text{II. 8})$$

Hence,

$$\Delta i_t = \left( \frac{V_s - V_{\text{out}}}{L} \right) DT \quad (\text{II. 9})$$

The preceding equation describes the variation in current within the circuit during the interval in which switch S1 remains in the closed state.

The second mode of operation begins when switch S2 opens, allowing the freewheeling diode, functioning as switch S1, to become conductive. At this stage, it is essential to examine the mechanism by which switch S1 conducts automatically. As previously discussed, during the first mode of operation, the inductor stores energy. When S<sub>2</sub> transitions to the open state, the inductor assumes the role of an energy source, releasing the energy accumulated in the preceding mode.

As a consequence of the polarity reversal across the inductor—an effect governed by Lenz's Law—the freewheeling diode transitions from a reverse-biased to a forward-biased state, thereby enabling current conduction. This ensures continuous current flow through the load, as depicted in the subsequent diagram.

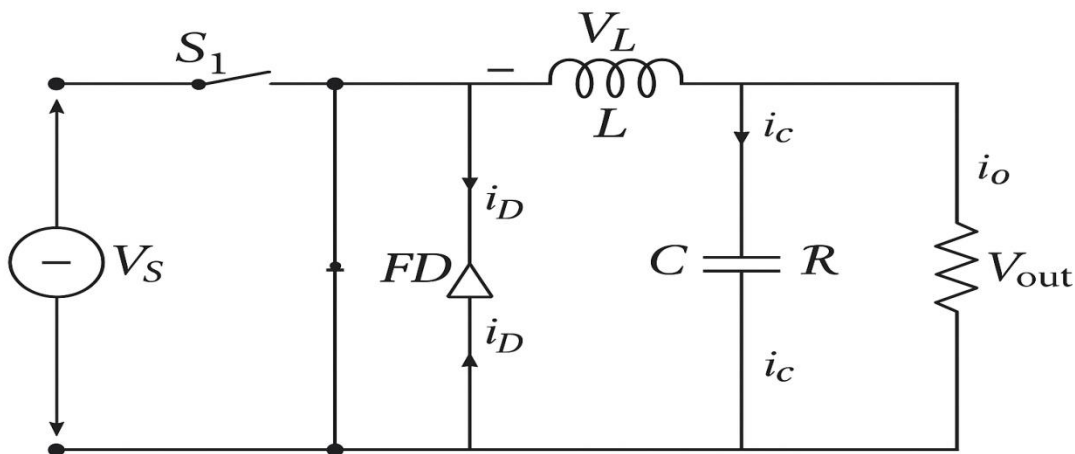


**Figure (II.5):** Buck Converter When S<sub>2</sub> is Closed

This current flow will continue until the energy stored in the inductor is completely dissipated. Once the inductor is fully discharged, the diode transitions to a reverse-biased state, leading to the opening of switch S2. Consequently, switch S1 closes immediately, and the cycle repeats.

Subsequently, Kirchhoff's Voltage Law (KVL) is applied to the circuit illustrated above.

$$0 = V_L + V_{\text{out}} \quad (\text{II. 10})$$

$$V_L = L \frac{di_L}{dt} = -V_{\text{out}} \quad (\text{II. 11})$$

Since, we know,

$$T = T_{\text{on}} + T_{\text{off}} \quad (\text{II. 12})$$

$$T = DT + T_{\text{off}} \quad (\text{II. 13})$$

$$T_{\text{off}} = T - DT \quad (\text{II. 14})$$

$$T_{\text{off}} = (1 - D)T \quad (\text{II. 15})$$

$$V_L = L \frac{\Delta i_L}{\Delta t} = -V_{\text{out}} \quad (\text{II. 16})$$

$$T_{\text{off}} = \Delta t = (1 - D)T \quad (\text{II. 17})$$

$$L \frac{\Delta i_L}{(1 - D)T} = -V_{\text{out}} \quad (\text{II. 18})$$

So,

$$\Delta i_L = -\frac{V_{\text{out}}}{L} (1 - D)T \quad (\text{II. 19})$$

This equation defines the rate of change of current through the inductor when switch S1 is in the open state.

It is a well-established principle that the net change in inductor current over an entire switching cycle is zero. Therefore,

$$\Delta i_{L(s1-closed)} + \Delta i_{L(s1-open)} = 0 \quad (\text{II. 20})$$

$$\frac{V_s - V_{\text{out}}}{L} DT + \left\{ -\frac{V_{\text{out}}}{L} (1 - D)T \right\} = 0 \quad (\text{II. 21})$$

On simplifying,

$$\frac{V_s DT}{L} - \frac{V_{\text{out}} DT}{L} - \frac{V_{\text{out}} T}{L} + \frac{V_{\text{out}} DT}{L} = 0 \quad (\text{II. 22})$$

$$\left( \frac{V_s DT}{L} \right) = \frac{V_{\text{out}} T}{L} \quad (\text{II. 23})$$

$$V_{\text{out}} = DV_s \quad (\text{II.24})$$

The following figure illustrates the waveform representation of a Buck Converter:

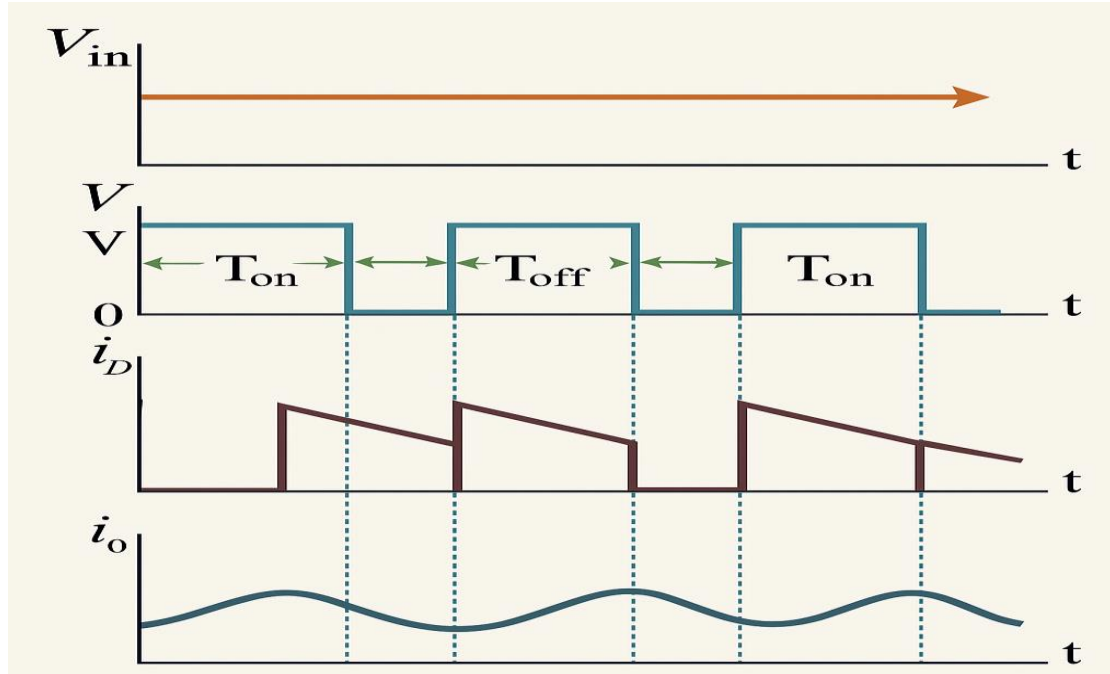


Figure (II.6): Wave form Representation

Therefore, it can be stated that buck converters are employed to obtain a reduced DC voltage level from a constant DC input source.

### Boost Converter:

Boost converters, also referred to as step-up DC-DC converters, represent a category of chopper circuits that deliver an output voltage exceeding the supplied input voltage. In these converters, the DC-to-DC conversion is carried out in such a manner that the resulting output voltage possesses a greater magnitude than the input voltage. The term 'boost' is attributed to this type of converter due to its characteristic function of increasing the input voltage to a higher output level.

### Operating Principle of Boost Converter

The figure given below is the circuit representation of the boost converter:

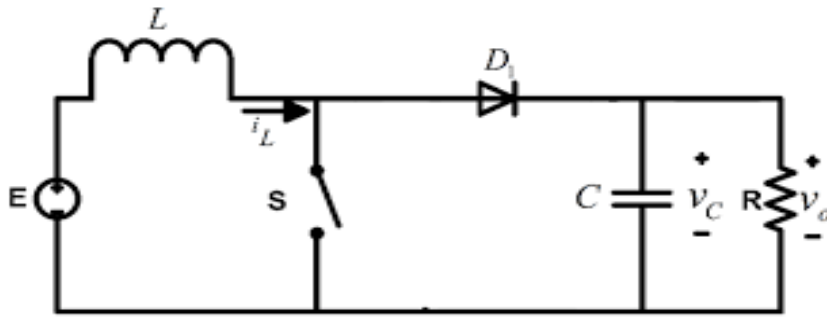


Figure (II.7):Elementary Circuit of Boost Converter

The circuit here is an elementary form of step-up DC-DC converter which necessarily requires a large inductor  $L$  in series connection with the voltage source. The whole circuit arrangement operates in a way that it helps in maintaining a regulated dc signal at the output.

Let us understand how the given circuit operates in order to provide an increased dc signal at the load.

Initially, when the chopper CH is in on state, then in the presence of supply dc input current begins to flow through the closed path of the circuit i.e., passing through the inductor as shown in the figure below.

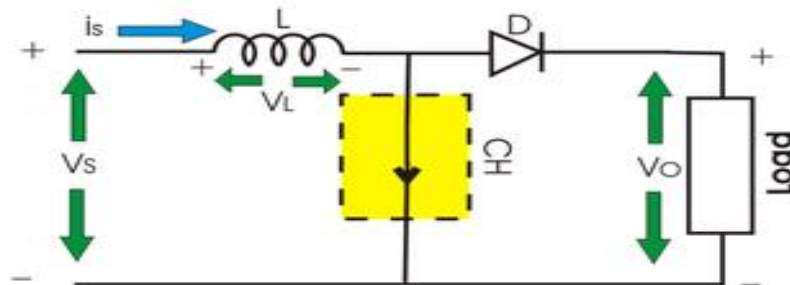


Figure (II.8):The Chopper CH is in on State

Here, the polarity of the inductor will be according to the direction of the flow of current. In this particular case, the diode in the configuration is in reverse biased condition and so current will not be allowed to flow through that particular part of the circuit during on state of the DC-DC converter. Resultantly, the voltage across DC-DC converter will appear across the load.

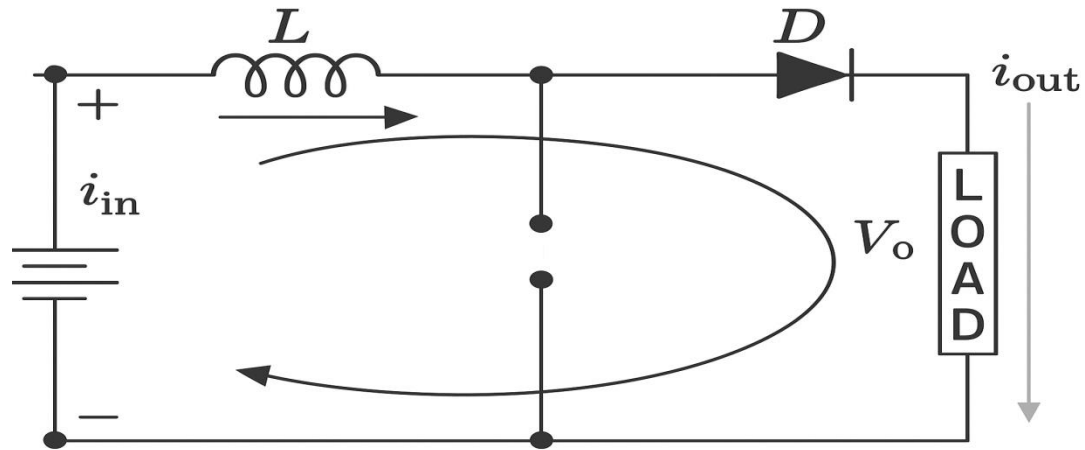


Figure (II.9): The Chopper CH is in Off State

Furthermore, at the instant when CH is in the off state, then the part of the circuit through which the current was flowing earlier will not be active in this case. However, as the inductor stores, the energy in the form of a magnetic field and so the current through it will not die out instantly.

Also, we know according to Lenz's law a reverse current will be induced that will oppose the cause which has produced it. And so, due to the induced current, the polarity of the inductor will get reversed. This reverse polarity of the inductor forward biases the diode present in the circuit. This provides the path for the current through the diode that flows through the load during the off state of the chopper i.e.,  $T_{off}$ . However, we must note here that the current through the inductor is of decreasing nature and will die out after a point in time.

Thus, the total voltage across the load will be given as:

$$V_{out} = V_{in} + V_L \quad (\text{II. 25})$$

This means that the output voltage exceeds the applied input voltage. Thus, performs step-up conversion as the energy stored within the inductor during the  $T_{on}$  period is released during the  $T_{off}$  period.

During the  $T_{on}$  period, the voltage across the inductor will be given as:

$$V_L = L \frac{di}{dt} \quad (\text{II. 26})$$

Let us have a look at the waveform representation of the step-up choppers shown below:

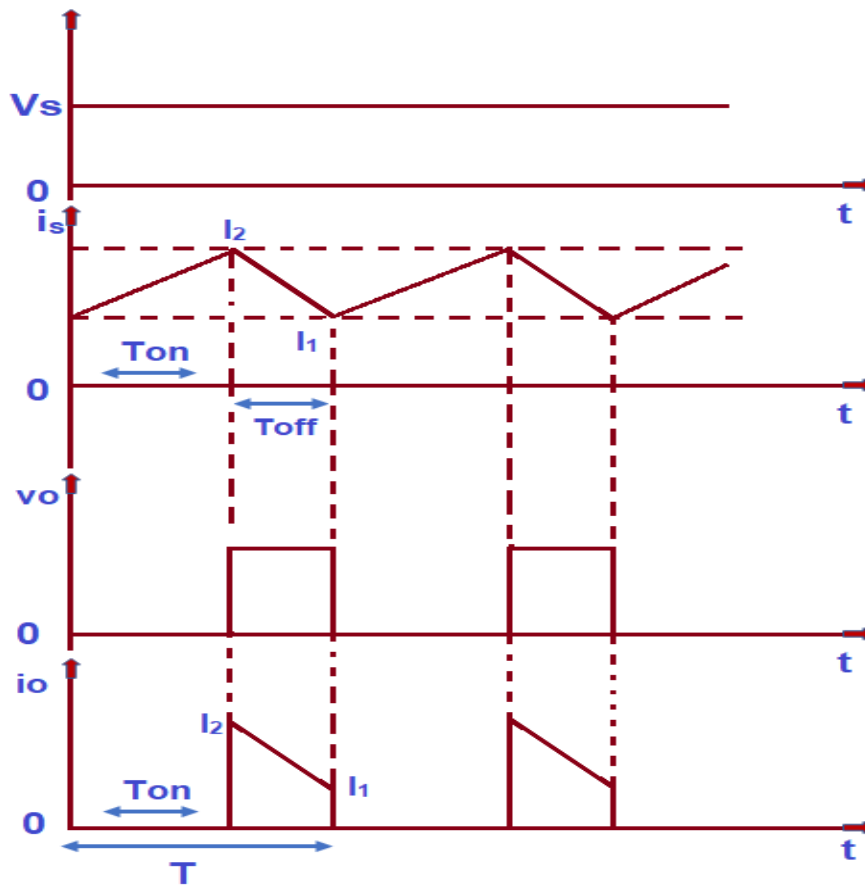


Figure (II.10): Waveform Representation

During the  $T_{on}$  period, the current flowing through the inductor transitions from  $i_1$  to  $i_2$ , as clearly depicted above. Similarly, during the  $T_{off}$  period, the inductor current decreases from  $i_2$  to  $i_1$ . Regarding voltage, during the turn-on period, the voltage across the inductor is equal to the supply input voltage. However, when the switch CH turns off, applying Kirchhoff's Voltage Law (KVL) to the circuit shown above yields the following results.

$$\text{so} \\ V_L - V_0 + V_{in} = 0 \quad (\text{II. 27})$$

This means,

$$V_L = V_0 - V_{in} \quad (\text{II. 28})$$

Given that the output current varies linearly, the energy input supplied by the source to the inductor when CH is in the ON state can be expressed as:

$W_{on} = (\text{voltage across the inductor})(\text{average current through the inductor})T_{on}$

$$W_{on} = V_{in} \left( \frac{i_1 + i_2}{2} \right) T_{on} \quad (\text{II. 29})$$

Further, the energy that the inductor releases to the load when CH is off is given as:

$W_{off} = (\text{voltage across the inductor})(\text{average current through the inductor})T_{off}$

$$W_{off} = V_{out} - V_{in} \left( \frac{i_1 + i_2}{2} \right) T_{off} \quad (\text{II. 30})$$

For a lossless system, comparing the two energies, we will have,

$$V_{in} \left( \frac{i_1 + i_2}{2} \right) T_{on} = V_{out} - V_{in} \left( \frac{i_1 + i_2}{2} \right) T_{off} \quad (\text{II. 31})$$

On simplifying,

$$V_{in} T_{on} = V_{out} T_{off} - V_{in} T_{off} \quad (\text{II. 32})$$

$$V_{out} T_{off} = V_{in} T_{on} + V_{in} T_{off} \quad (\text{II. 33})$$

$$V_{out} T_{off} = V_{in} (T_{on} + T_{off}) \quad (\text{II. 34})$$

Since we know,  $T = T_{on} + T_{off}$ , therefore,

$$V_{out} T_{off} = V_{in} T \quad (\text{II. 35})$$

$$V_{out} = V_{in} \frac{T}{T_{off}} \quad (\text{II. 36})$$

$$V_{out} = V_{in} \frac{T}{T - T_{on}} \quad (\text{II. 37})$$

$$\begin{aligned} V_{out} \\ = V_{in} \frac{1}{\left( \frac{T}{T} - \frac{T_{on}}{T} \right)} \end{aligned} \quad (\text{II. 38})$$

Since, we know, duty cycle i.e.,  $\alpha = T_{on}/T$

$$V_{out} = V_{in} \frac{1}{(1 - \alpha)} \quad (\text{II. 39})$$

Thus, it can be concluded that the average load voltage can be increased by adjusting the duty cycle..

### II.4.3. Buck-Boost Converter:

The buck-boost converter is a type of DC-to-DC converter capable of producing an output voltage magnitude that can be either greater or less than the input voltage magnitude. It is utilized for "stepping up" DC voltage, analogous to how a transformer operates in AC circuits. Functionally, it is equivalent to a fly-back converter but employs a single inductor instead of a transformer. Among the various types of DC-DC converters, commonly referred to as choppers, the buck-boost converter is particularly versatile. This converter can operate as either a step-down or step-up converter, depending on its duty cycle, denoted as DA typical buck-boost converter circuit is illustrated below.

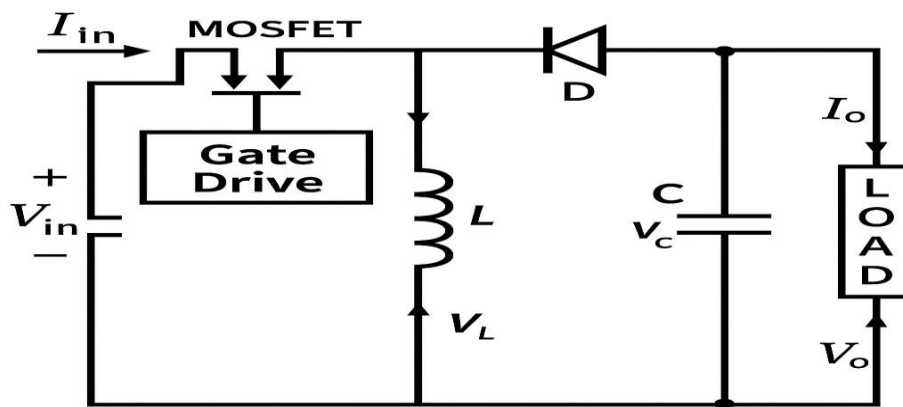


Figure (II.11): The Circuit Representation of Buck-Boost Converter

The input voltage source is connected to a solid-state switching device, while the second switching component used in the circuit is a diode. The diode is oriented in reverse relative to the direction of power flow from the source and is connected to both a capacitor and the load, with these components arranged in parallel, as illustrated in the figure above.

In this converter, the controlled switch operates using Pulse Width Modulation (PWM) to toggle between the ON and OFF states. PWM can function based on either time or frequency; however, time-based modulation is the more commonly employed approach. While frequency-based modulation offers versatility, it has the drawback of requiring a broad frequency range to precisely regulate the switch and achieve the desired output voltage.

Time-based modulation is predominantly utilized in DC-DC converters due to its simplicity in design and implementation. In this modulation technique, the switching frequency remains constant. The Buck-Boost converter operates in two distinct modes, the first of which occurs when the switch is in the ON state and conducting.

**Mode I: Switch is ON, Diode is OFF**

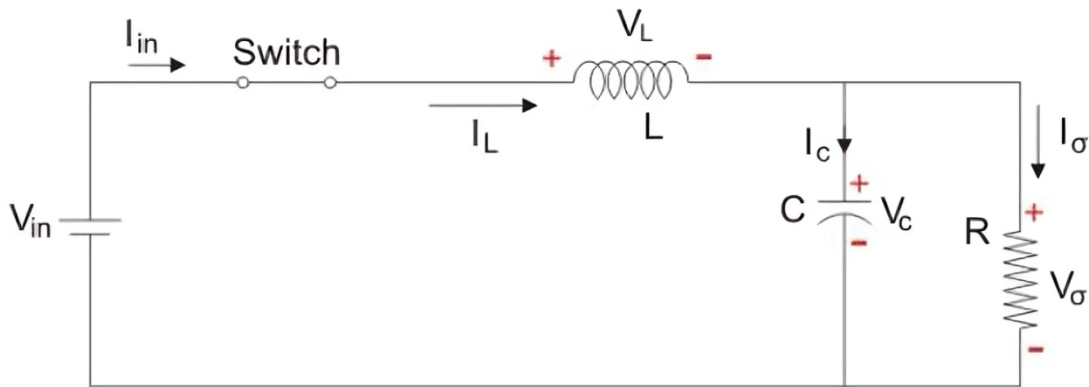


**Figure (II.12):** The Equivalent Circuit of Mode I

When the switch is in the ON state, it ideally behaves as a short circuit, offering zero resistance to current flow. Consequently, during this period, all the current flows through the switch and the inductor, returning to the DC input source.

During the ON state, the inductor stores energy. When the solid-state switch turns OFF, the polarity of the inductor reverses, allowing current to flow through the load, the diode, and back to the inductor. However, the direction of current flow through the inductor remains unchanged.

Let  $T_{on}$  represent the duration for which the switch remains ON, and  $T_{off}$  denote the duration for which it remains OFF. The total time period,  $T$ , is defined as:

$$T = T_{ON} + T_{OFF} \quad (\text{II. 40})$$

and the switching frequency:

$$f_{\text{switching}} = \frac{1}{T} \quad (\text{II. 41})$$

Let us now define another term, the duty cycle:

$$D = \frac{T_{ON}}{T} \quad (\text{II. 42})$$

Let us analyse the Buck Boost converter in steady state operation for this mode using KVL.

$$\begin{aligned} V_{in} &= V_L \\ V_L &= L \frac{di_L}{dt} = V_{in} \\ \frac{di_L}{dt} &= \frac{\Delta i_L}{\Delta t} = \frac{\Delta i_L}{DT} = \frac{V_{in}}{L} \end{aligned} \quad (\text{II. 43})$$

Since the switch is closed for a time  $T_{ON} = DT$  we can say that  $\Delta t = DT$ .

$$(\Delta i_L)_{\text{closed}} = \left( \frac{V_{in}}{L} \right) DT \quad (\text{II. 44})$$

When analyzing the Buck-Boost converter, it is essential to consider the following:

The inductor current remains continuous, which is ensured by selecting an appropriate inductance value (L).

In steady-state operation, the inductor current increases with a positive slope, reaching its maximum value during the ON state. Subsequently, during the OFF state, the current decreases with a negative slope, returning to its initial value. As a result, the net change in inductor current over a complete cycle is zero.

**Mode II:** Switch is OFF, Diode is ON

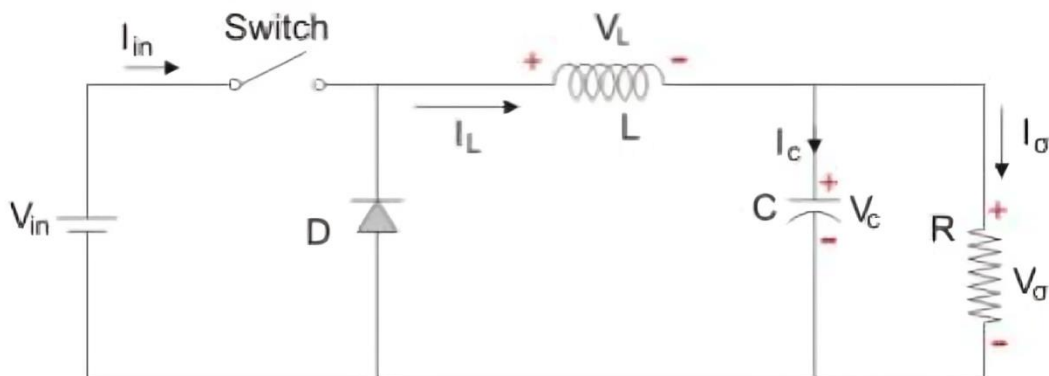


Figure (II.13): The Equivalent Circuit of Mode II

this mode, the polarity of the inductor reverses, and the energy previously stored in the inductor is released, ultimately being dissipated in the load resistance. This process helps sustain the current flow in the same direction through the load while also increasing the output voltage, as the inductor functions as an additional energy source alongside the input source. However, for analytical purposes, the original conventions are maintained to facilitate circuit analysis using Kirchhoff's Voltage Law (KVL). Buck Boost Converter Formula

Let us now analyse the Buck Boost converter in steady state operation for Mode II using KVL.

$$V_L = V_o \quad (\text{II. 45})$$

$$V_L = L \frac{di_L}{dt} = V_o \quad (\text{II. 46})$$

$$\frac{di_L}{dt} = \frac{\Delta i_L}{\Delta t} = \frac{\Delta i_L}{(1-D)T} = \frac{V_o}{L} \quad (\text{II. 47})$$

Since the switch is open for a time

$$T_{OFF} = T - T_{ON} = T - DT = (1-D)T \quad (\text{II. 48})$$

we can say that

$$\Delta t = (1-D)T \quad (\text{II. 49})$$

$$(\Delta i_L)_{open} = \left(\frac{V_o}{L}\right) (1-D)T \quad (\text{II. 50})$$

It is already established that the net change of the inductor current over any one complete cycle is zero.

$$(\Delta i_L)_{closed} + (\Delta i_L)_{open} = 0 \quad (\text{II. 51})$$

$$\left(\frac{V_o}{L}\right) (1-D)T + \left(\frac{V_{in}}{L}\right) DT = 0 \quad (\text{II. 52})$$

$$\frac{V_o}{V_{in}} = \frac{-D}{1-D} \quad (\text{II. 53})$$

It is known that the duty cycle (D) varies between 0 and 1. When  $D > 0.5$ , the output voltage exceeds the input voltage, whereas when  $D < 0.5$ , the output voltage is lower

than the input voltage. However, if  $D = 0.5$ , the output voltage is equal to the input voltage[22].

### II.5. Comparison of Converter Types:

Table (II.1) presents a summary of the voltage gains and switch stresses associated with different types of converters. For these converters, the variation of voltage gain as a function of the duty cycle is illustrated. While several converter types can be classified as boost converters, particularly when the duty cycle exceeds 0.5, only the conventional boost converter maintains a voltage-boosting capability across the entire duty cycle range. For instance, at a duty cycle of 0.5, the boost converter produces an output voltage that is twice the input voltage. In contrast, for other boost-derived converters, the output voltage equals the input voltage at this duty cycle value. It is only when the duty cycle approaches 1 that these boost-derived converters begin to exhibit behavior similar to that of the conventional boost converter[23].

Converter /Parameters	Voltage Gain $\frac{V_{out}}{V_{in}}$	Voltage Controls $V_{k,max} =  V_{d,max} $	Current Controls $i_{k,max} = V_{d,max} = i_{d,max}$
<b>Boost</b>	$\frac{1}{1-\alpha}$	$\frac{V_{in}}{1-\alpha} + \frac{\Delta V_{out}}{2}$	$\frac{I_{out}}{1-\alpha} + \frac{\Delta I_L}{2}$
<b>Buck</b>	$\frac{\alpha}{1-\alpha}$	$\frac{V_{in}}{1-\alpha} + \frac{\Delta V_{out}}{2}$	$\frac{VC}{1-\alpha} + \frac{\Delta V_{out}}{2}$
<b>Buck-Boost</b>	$\alpha$	$V_{in}$	$i_L + \frac{\Delta I_L}{2}$

Table (II.1): Comparison of Converter Types.

### II.6. Efficiency of Static Converters:

The table provides insight into the efficiency of some well-known converter types[24].

Structure	Conversion Efficiency	Battery
Boost	92%	24V
Buck	93%	12V
Buck-Boost	92%	12-24V

Table (II.2): Efficiency of Static Converters.

**II.7. Conclusion:**

In conclusion, DC-DC converters play a pivotal role in modern electronics by enabling efficient power management through the conversion of one voltage level to another. With various types, including buck, boost, and buck-boost converters, they provide versatility in meeting the diverse voltage requirements of different electronic systems.

These converters are widely utilized across multiple industries, including automotive, renewable energy, telecommunications, and consumer electronics. Their applications range from powering small electronic devices to regulating energy flow in solar power systems, making them indispensable in contemporary technology.

Additionally, Maximum Power Point Tracking (MPPT) is a crucial technology, particularly in renewable energy systems such as solar power. It optimizes energy extraction from photovoltaic (PV) panels by dynamically adjusting the electrical operating point to maximize power output. In the following chapter, we will explore MPPT, its significance, and various implementation methods in greater detail.

# **Chapter III**

**Maximum Power**

**Point Tracking**

### III.1. Introduction:

To address the performance limitations of photovoltaic (PV) panels and attain maximum efficiency, it is imperative to optimize the design of all components within the PV system. This includes the enhancement of DC/DC converters, which serve as the interface between the PV generator and the load, in order to facilitate continuous extraction of maximum power. This is achieved through the implementation of a Maximum Power Point Tracking (MPPT) controller, which enables the system to operate consistently at its maximum power point (MPP) without incurring energy transfer losses. As a result, optimal power output is maintained under dynamic load conditions and varying atmospheric parameters such as irradiance and temperature.

Since the 1970s, a wide range of MPPT control strategies have been developed—ranging from basic methods relying on feedback from voltage and current measurements to more advanced techniques that utilize algorithms to compute the MPP of the PV system. Among the most widely adopted MPPT algorithms are the Incremental Conductance (INC) method, the Perturb and Observe (P&O) method, and the hill-climbing technique[25].

### III.2. Maximum Power Point Tracking:

Enhancing the efficiency of photovoltaic (PV) systems necessitates the maximization of power output from the PV generator. This objective can be realized by accurately selecting the operating point, thereby aligning the load impedance with the voltage source. In this context, the DC-DC converter functions as an impedance matching device, ensuring that the PV system operates at the optimal point, which facilitates the extraction of maximum power from the generator[26].

Accordingly, maximizing the power output of a PV source involves identifying and maintaining this optimal operating point through a control process known as Maximum Power Point Tracking (MPPT). MPPT techniques employ iterative search algorithms to determine the solar module's operating point that yields the highest possible power output without interrupting system functionality. These algorithms are based on the continuous optimization of the power produced by PV modules. The extracted power is computed using real-time measurements of the module's current and voltage, with

the power determined as the product of these two parameters. Various MPPT methods utilize these measurements to track and maintain operation at the actual Maximum Power Point (MPP).

Several MPPT strategies exist, including the constant voltage method, constant current method, incremental conductance algorithm, and the perturb and observe (P&O) method. In the present work, the perturb and observe method is employed due to its simplicity and ease of implementation.

### **III.3. Working principle of MPPT:**

Specific control strategies have been developed to enable systems to operate at the maximum point of their characteristic curves, even when these points are not known a priori, and without requiring knowledge of when or why these points may have shifted. In the context of energy sources, this corresponds to the identification and tracking of maximum power points. Such control approaches are commonly referred to in the literature as Maximum Power Point Tracking (MPPT) .

The fundamental principle of MPPT control lies in continuously searching for the Maximum Power Point (MPP) while ensuring optimal matching between the generator and its load, thereby facilitating the transfer of maximum power. To simplify the implementation conditions of this control strategy, a direct current (DC) load is typically selected. As illustrated in this configuration, MPPT control is inherently associated with a four-terminal network (or four-pole) that provides the necessary degrees of freedom to achieve impedance matching between the photovoltaic (PV) generator and the load[27].

In photovoltaic energy conversion systems, this four-pole is generally realized through the use of a DC-DC converter. The role of the converter is to ensure that the power delivered by the PV generator corresponds to its maximum available power ( $P_{MAX}$ ), which can then be efficiently transferred to the connected load.

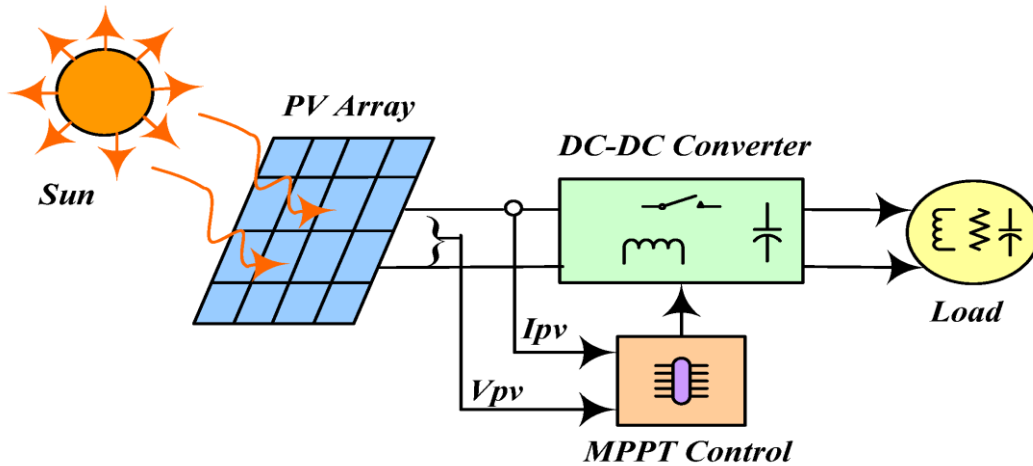


Figure (III.1): Block Diagram of The PV System

A commonly employed control strategy involves the automatic adjustment of the duty cycle to maintain the generator at its optimal operating point, particularly in response to sudden load variations that may occur unpredictably. Figure (III.2) illustrates three distinct types of disturbances. Depending on the nature of the disturbance, the operating point may shift from the initial maximum power point (MPP1) to a new operating point (P1), which may deviate to varying degrees from the optimal condition.

In the case of solar irradiance variation (case a), it is necessary to modify the duty cycle to enable convergence toward the new maximum power point (MPP2). In the event of a load variation (case b), the operating point may shift, but the system can reestablish a new optimal position through appropriate control actions. Lastly, a variation in the operating point may also arise—though to a lesser extent—from changes in the photovoltaic module's operating temperature (case c). While control intervention remains necessary in this scenario, the temporal response requirements are less stringent compared to those in the previous two cases[28].

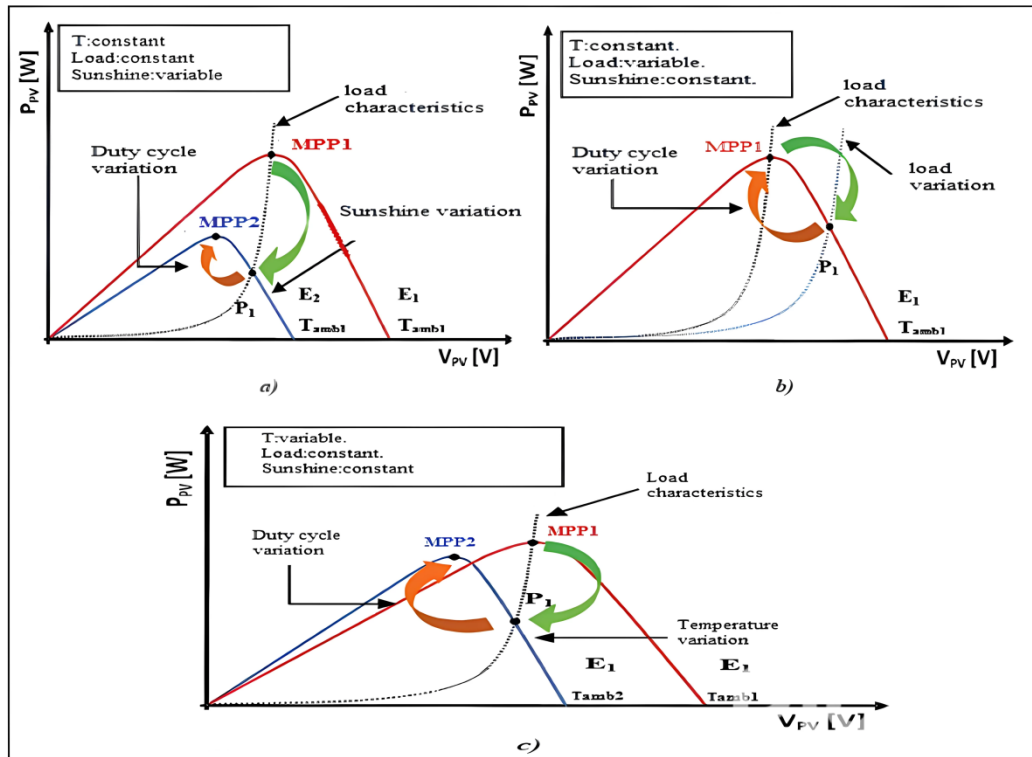


Figure (III.2): Search and Recovery Of MPP

#### III.4. Classification of MPPT Control:

Maximum Power Point Tracking (MPPT) controllers are commonly classified according to their electronic implementation, which may be analog, digital, or a hybrid of both. However, a more meaningful and functional classification is based on the nature of the search algorithm they employ and the specific input parameters used to facilitate the tracking of the maximum power point..

##### III.4.1. Classification of MPPT Controllers Based on Input Parameters:

###### a) MPPT Controllers Operating from Input Parameters:

Several MPPT controllers operate by tracking the maximum power point based on the variation of power supplied by the photovoltaic (PV) array. Among these are techniques such as the Perturb and Observe (P&O) method and incremental conductance algorithms, which utilize the power output of the PV array to determine and apply appropriate control actions for MPP tracking. Additionally, some controllers rely on

proportional relationships between the optimal parameters associated with the maximum power point ( $V_{opt}$  and  $I_{opt}$ ) and the characteristic parameters of the PV module ( $V_{oc}$  and  $I_{sc}$ ).

Notably, MPPT controllers inspired by neural network architectures also fall within this category. These controllers may either utilize extensive memory systems that store a comprehensive set of possible scenarios or employ approximate models to infer control actions. All controllers in this category are characterized by their high precision and rapid dynamic response[29].

#### **b) MPPT Controllers Operating from Output Parameters of the Converter:**

The literature also reports the development of algorithms that utilize the output parameters of DC-DC converters for Maximum Power Point Tracking (MPPT). For instance, certain MPPT controllers aim to maximize the output current, a strategy commonly applied when the load consists of a battery. In systems employing output-based parameters, an estimation of the maximum power point ( $P_{max}$ ) is inferred through the efficiency of the converter. In essence, the higher the efficiency of the conversion stage, the more accurate this approximation becomes. Nevertheless, systems that rely on a single sensor are generally characterized by lower precision. Notably, many of these methods were originally developed for space applications[29].

### **II.4.2. Classification of MPPT Controllers According to the Type of Search:**

#### **a) Indirect MPPT:**

This form of Maximum Power Point Tracking (MPPT) control leverages the existing relationship between the measured variables (such as open-circuit voltage,  $V_{oc}$ ), which can be readily determined, and the estimated location of the Maximum Power Point (MPP). It also incorporates control strategies based on the estimation of the photovoltaic (PV) system's operating point derived from a predefined parametric model. Additionally, some controls optimize voltage tracking by solely accounting for variations in cell temperature, as measured by a sensor. These control methods are advantageous due to their simplicity in implementation and are primarily designed for cost-effective, low-precision systems operating in regions characterized by minimal climatic variation[30].

**b) Direct MPPT:**

This MPPT control method determines the optimal operating point (Maximum Power Point, MPP) based on the system's measured currents, voltages, or power outputs, allowing it to respond to unpredictable variations in the photovoltaic (PV) system's performance. Typically, these procedures employ a search algorithm that identifies the maximum power point on the curve without interrupting the system's operation. In practice, the operating point voltage is incremented at regular intervals; if the output power increases, the search direction is maintained for the subsequent step, whereas if the power decreases, the direction is reversed. As a result, the actual operating point oscillates around the MPP. This fundamental approach can be preserved by other algorithms to mitigate potential errors in interpretation, which may arise, for example, from a misdirected search caused by an increase in power due to rapid changes in radiation levels. To determine the PV generator's power—an essential component in locating the MPP—both the generator's voltage and current must be measured and then multiplied. Some alternative algorithms involve introducing small-signal sinusoidal variations in the converter's switching frequency to compare the alternating and direct components of the PV system's voltage, thereby positioning the operating point as close as possible to the MPP. The primary advantage of this type of control lies in its precision and rapid responsiveness[30].

**III.5. Different MPPT Commands Synthesis:**

Numerous studies on MPPT algorithms have been published consistently in the literature since 1968, the year the first command law adapted for renewable energy (specifically photovoltaic systems) was introduced. Due to the extensive volume of publications in this area, a classification of different MPPT techniques has been established based on their underlying principles..

**III.5.1. First MPPT Commands Types:**

The algorithm implemented in the first MPPT command was relatively simple. Indeed, the capacity of microcontrollers available at that time was low and applications, especially, for space had fewer constraints regarding temperature and solar irradiation. The first command to be applied to a photovoltaic system was described by A.F. Boehringer. The command was based on an algorithm of adaptive control, to maintain the system at its maximum power point PPM. This is described in Figure 3 and can be

easily implemented on a computer. The system calculates the power at time  $t_i$  from the measurements of  $I_{PV}$  and  $V_{PV}$ , and compares it to the one stored in memory (time  $t_{i-1}$ ). From there, a new duty cycle  $D$  is calculated and applied to the static converter.

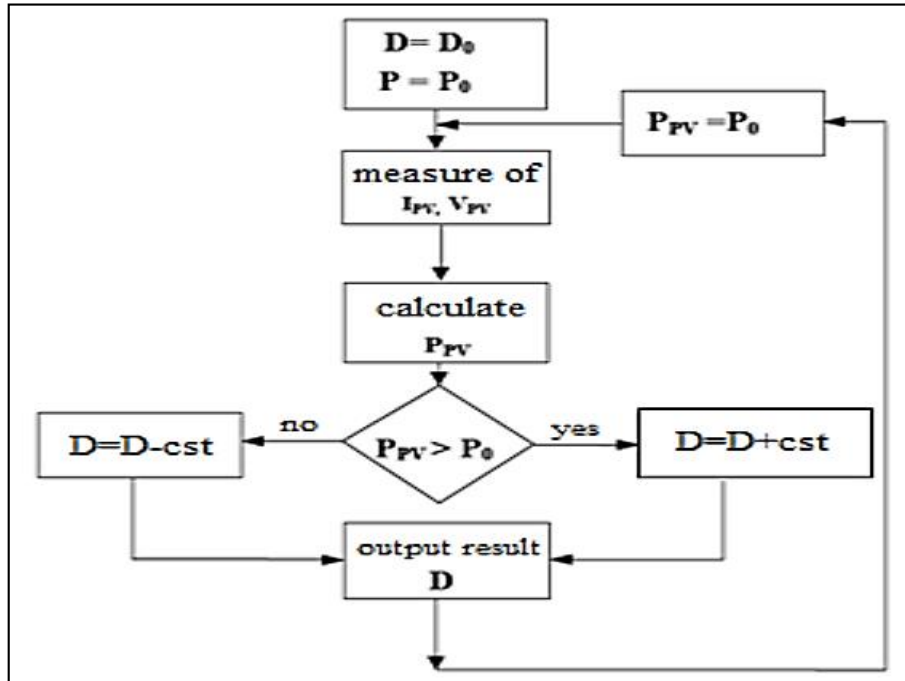


Figure (III.3): Bloc Diagram of a Digital MPPT Command

This principle remains valid from a theoretical perspective and continues to be applied to more efficient numerical algorithms. However, both the response time and the accuracy of the Maximum Power Point (MPP) search have been significantly improved[28].

### III.5.2. Efficient MPPT Commands Algorithms:

The four methods most commonly encountered are typically referred to as Hill Climbing, Perturb & Observe, Incremental Conductance, and Artificial Neural Networks.

#### III.5.2.1. Algorithm Perturb and Observe (P&O):

The principle of MPPT commands of the Perturb & Observe (P&O) type involves perturbing the voltage  $V_{pv}$  with a small amplitude around its initial value and analyzing the resulting variation in power  $P_{pv}$ . As illustrated in Figure (III.4), it can be inferred that if a positive increment in  $V_{pv}$  leads to an increase in  $P_{pv}$ , the operating point lies to the left of the Maximum Power Point (MPP). Conversely, if the power decreases, it indicates that the system has surpassed the MPP..

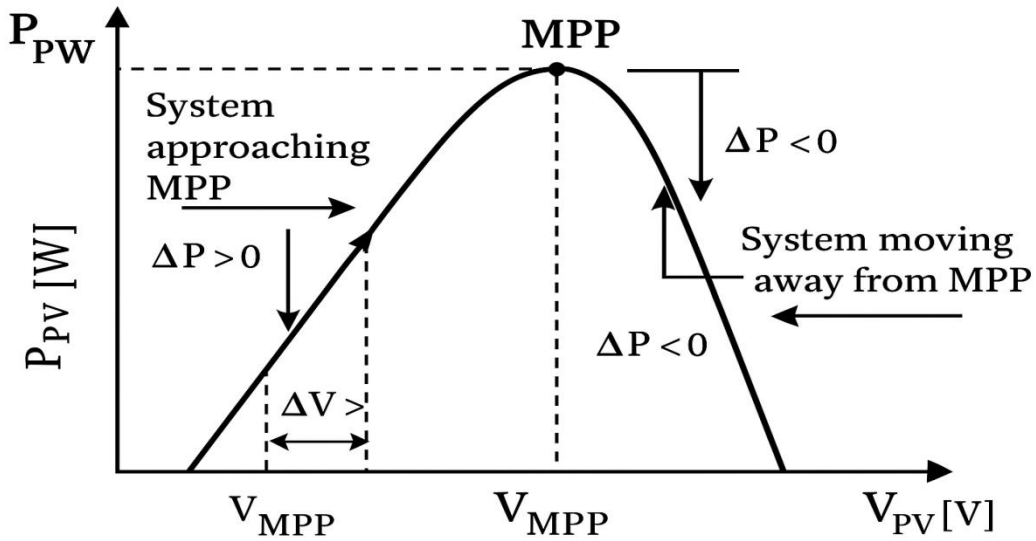


Figure (III.4): Ppv VS Vpv Characteristic of a Solar Panel

Figure (III.5) illustrates the algorithm employed in a conventional Maximum Power Point Tracking (MPPT) approach of the Perturb and Observe (P&O) type, wherein the evolution of power is evaluated following each voltage perturbation. This method requires the use of two sensors current and voltage to continuously determine the instantaneous power output of the photovoltaic generator. The P&O algorithm is widely adopted due to its simplicity and ease of implementation. Nevertheless, it presents certain limitations, notably the oscillations around the Maximum Power Point (MPP) in steady-state conditions. These oscillations arise from the algorithm’s periodic search for the MPP, which causes the operating point to fluctuate continuously around the optimal value.

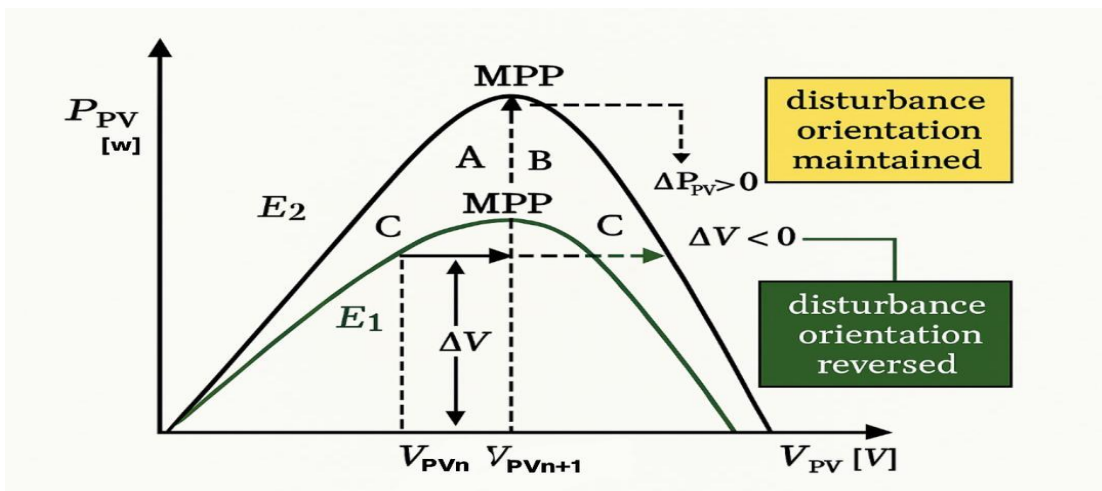
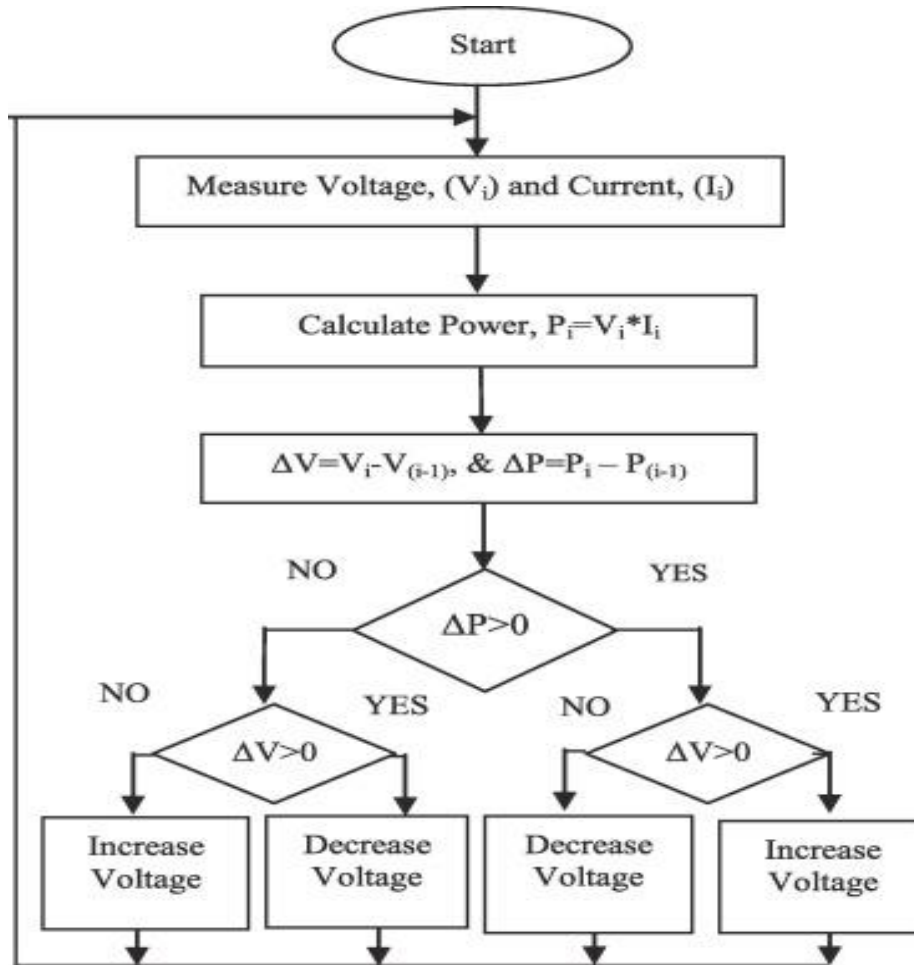


Figure (III.5): Divergence of The P & O Command Due to Radiation Variations

Figure (III.6) shows a detailed algorithm of the P & O command.



**Figure (III.6):** Algorithm of The P & O Type of Command

To elucidate this concept, consider the example of a given solar irradiation level, denoted as  $E1$  with an initial operating point located at position A. Following a voltage disturbance of magnitude  $\Delta V$ , the operating point shifts to position B. This shift indicates a variation in the operating condition under non-illuminated conditions and a reversal in the sign of the disturbance. The reversal is attributed to the detection of a negative derivative of the power, which subsequently leads to oscillations around the maximum power point (MPP). These oscillations result from the trajectory of the operating point between positions B and C. It is important to note that the associated power transfer losses will vary in magnitude depending on the relative positions of points B and C with respect to point A. Upon changing the irradiation level from  $E1$  to  $E2$ , the operating point transitions from A to D, which, in this context, is interpreted as a positive variation in power[28].

### III.5.2.2. Algorithm Hill Climbing:

The principal advantage of the hill-climbing Maximum Power Point Tracking (MPPT) method lies in its simplicity. This technique utilizes the duty cycle of the boost converter as a feedback parameter during the execution of the MPPT process. However, a primary limitation of this method arises from the trade-off between system stability under conditions of constant irradiation. An additional drawback is its limited responsiveness to abrupt changes in solar radiation. During periods of steady irradiation, it is necessary to employ a very small variation in the duty cycle, denoted as  $\Delta D$ , in order to minimize significant oscillations in power around the maximum power point, which would otherwise reduce the energy harvested by the photovoltaic (PV) system. Conversely, in situations of rapidly changing irradiation, a larger variation in the duty cycle is required to expedite the tracking of the maximum power point[31],[32].

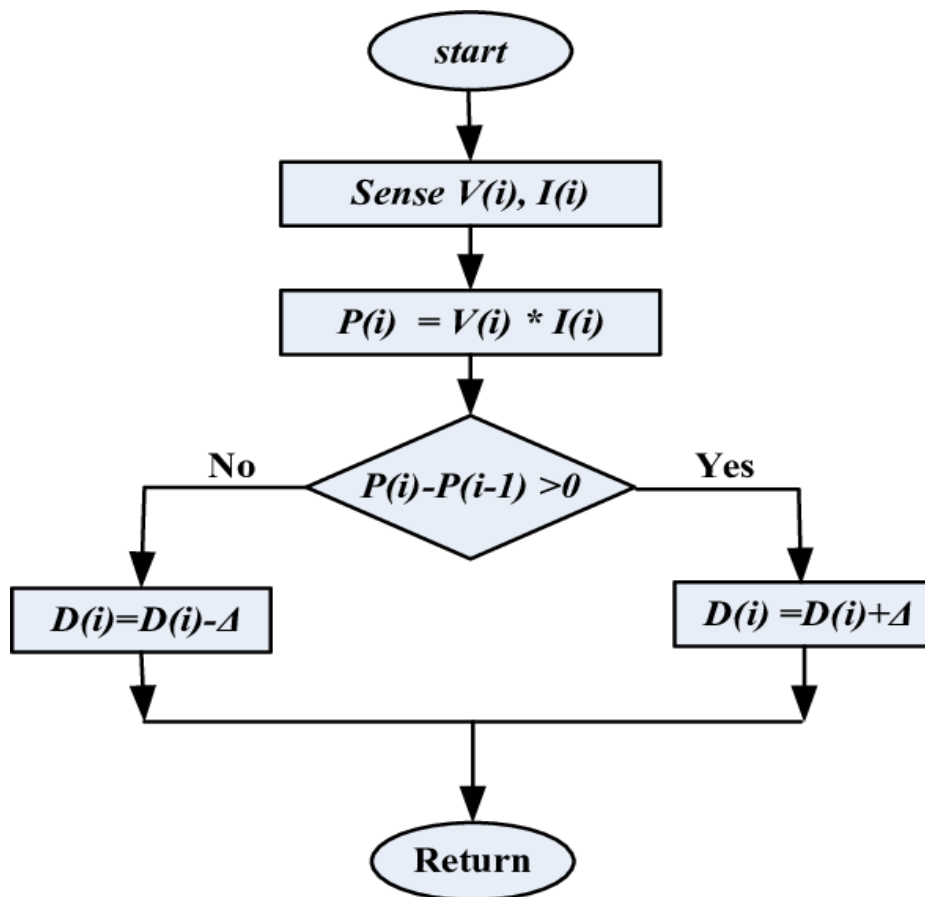


**Figure (III.7):** State Flowchart of Hill Climbing MPPT Technique.

### III.5.2.3. Algorithm Incremental conductance (INC):

The principle of this algorithm is based on knowledge of the conductance value  $G=I/V$  and the conductance increment ( $dG$ ) in order to deduce the position of the operating point relative to the maximum power point. If the conductance increment ( $dG$ ) is greater than the negative of the conductance ( $-G$ ), the duty cycle is decreased. On the other hand, if the conductance increment is less than the negative of the conductance, the duty cycle is increased. This process is repeated until the maximum power point is reached[33].

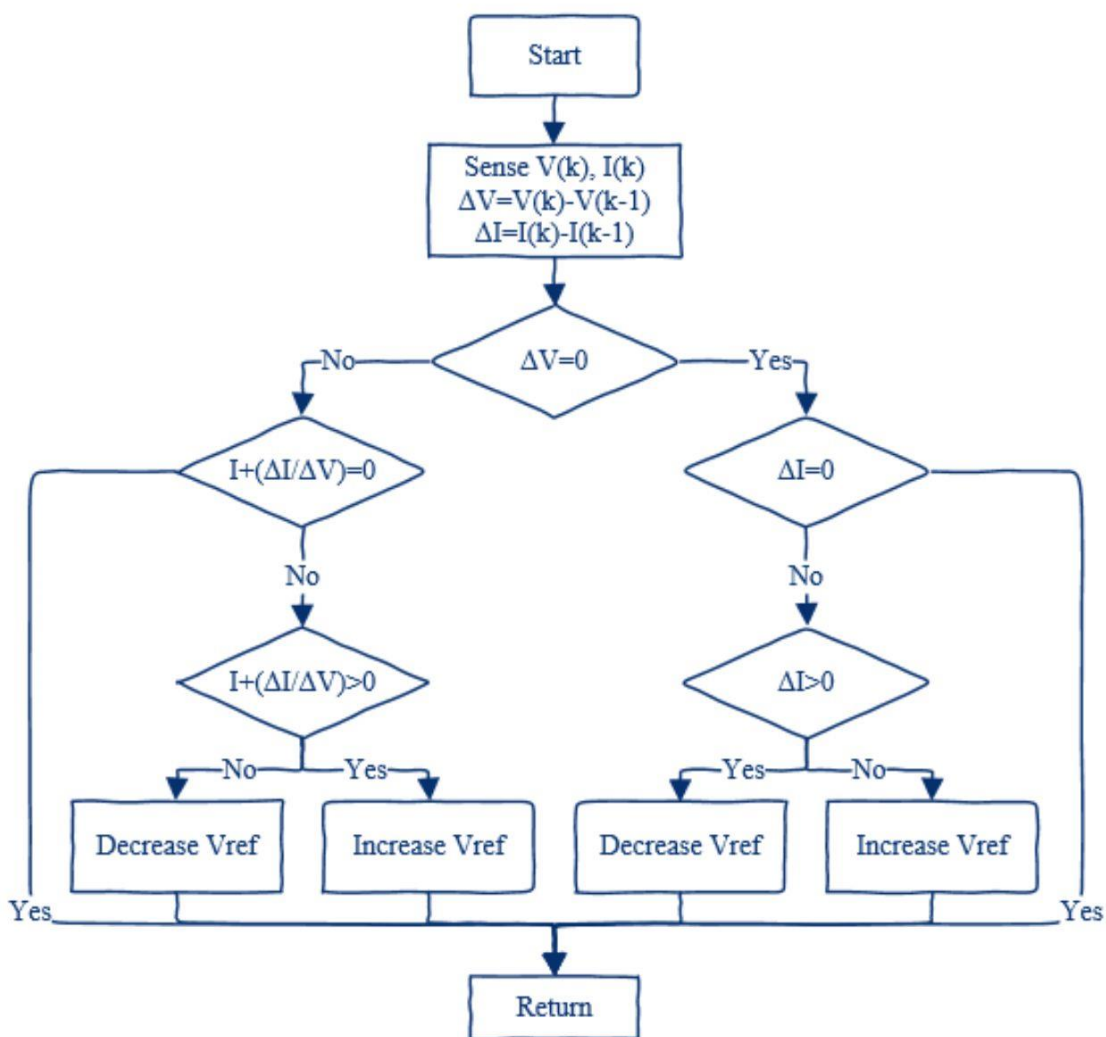
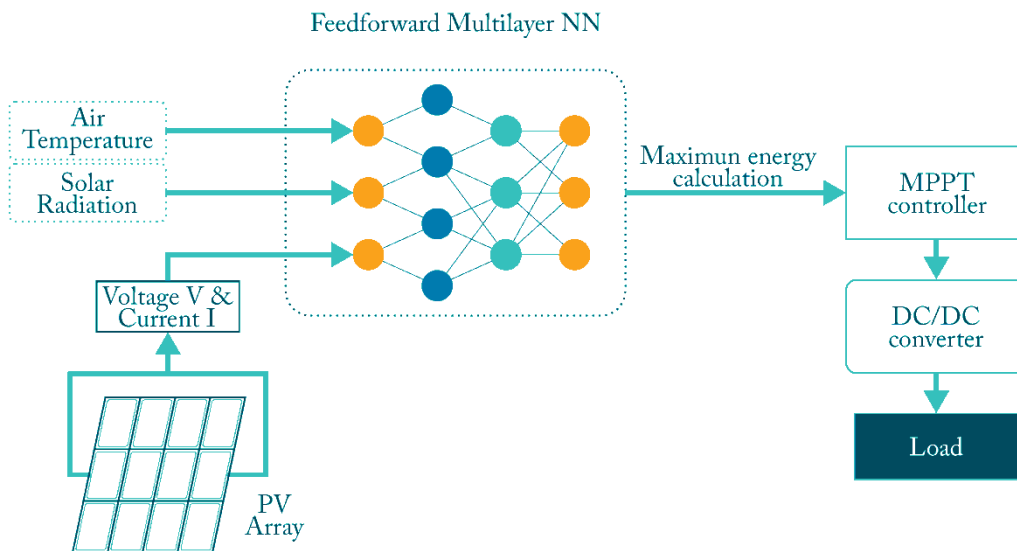


Figure (III.8): Flowchart for The Incremental Conductance Algorithm.

### III.5.2.4. Artificial Neural Networks (ANN):

Generally, an artificial neural network utilizes numerous processors working simultaneously and arranged in different layers. The initial layer takes in raw data inputs, similar to how the optic nerves receive visual information in humans.

Afterward, each subsequent layer receives the processed outputs from the previous layer. This process resembles the human experience, where neurons receive signals from neurons closer to the optic nerve. The final layer, however, generates the system's ultimate results or outputs.



**Figure (III.9):** Functioning of Artificial Neural Networks

Neural networks enable computers to learn from new data through algorithms. Computers with neural networks are trained on labeled example data to learn tasks like object recognition by analyzing patterns in the examples. Unlike traditional algorithms, neural networks cannot be directly programmed - they learn in a similar way to a child's developing brain. There are three main learning methods:

1. **Supervised Learning:** The algorithm trains on labeled data and adjusts until it can achieve the desired output.
2. **Unsupervised Learning:** The network analyzes unlabeled data, with a cost function guiding it towards the desired result by indicating deviations.

- 3. Reinforcement Learning:** The network is rewarded for positive results and penalized for negative ones, enabling it to learn and improve over time like humans learn from mistakes.

#### **III.5.2.4.1. Application of Artificial Neural Networks in MPPT:**

Artificial neural networks are employed to optimize maximum power point tracking (MPPT), a crucial element in photovoltaic (PV) systems. They improve the efficiency of capturing solar energy by continuously adjusting the operating point of the PV panels to maximize their power output. This adjustment accounts for changing environmental factors like solar radiation levels, temperature, and shading conditions. By doing so, neural network-based MPPT enables PV systems to more effectively harness solar energy and increase their overall energy production.

This example shows the use and practical application of artificial neural networks and their valuable role in improving the performance of PV systems through MPPT algorithms[34].

#### **III.5.2.4.2. Implementation of ANN in MATLAB/SIMULINK :**

The Neural Network Fitting app in MATLAB provides a user-friendly interface for designing, training, and evaluating artificial neural networks. The process involves selecting the data, configuring the network architecture, training the network, and assessing its performance through various plots and metrics. This tool is particularly useful for tasks like MPPT, where accurate modeling of complex relationships between inputs and outputs is crucial.

##### **1. Data Collection:**

The initial phase of the proposed method involves collecting data from MPPT method simulations performed under a variety of scenarios. Data collection is the cornerstone for training and evaluating the ANN-based MPPT model[20].

##### **2. Setting Up the Neural Network Fitting Tool:**

To begin the implementation process, we will open the Neural Network Fitting Tool in MATLAB. This tool provides a user-friendly interface for training and evaluating neural networks. We will import our defined variables and configure the tool for our specific application[35].

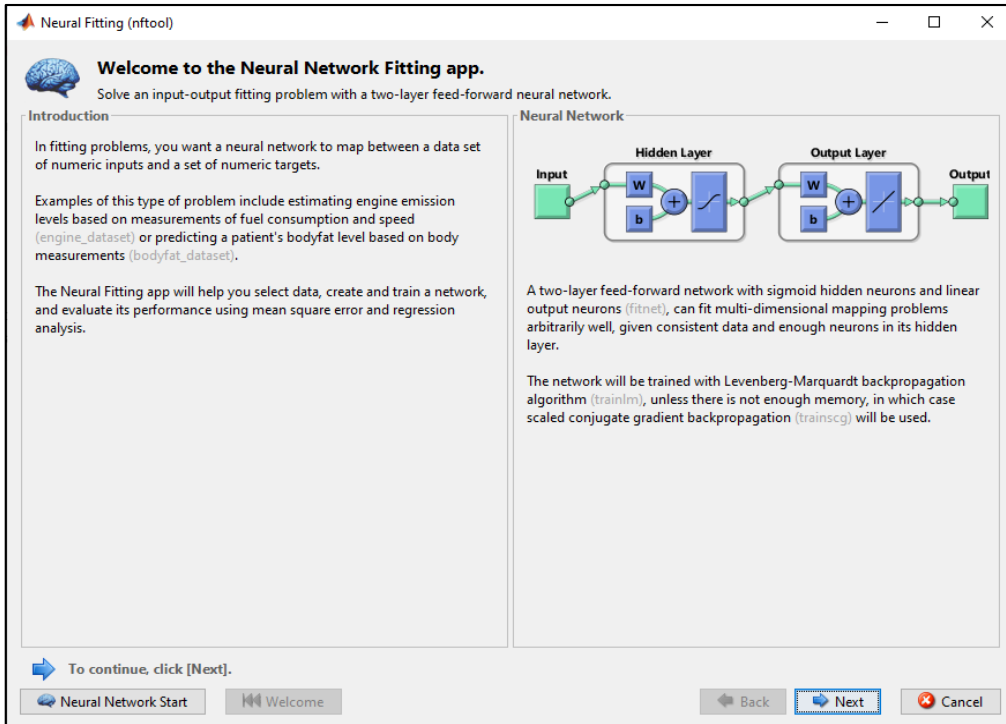


Figure (III.10): Setting Up the Neural Network Fitting Tool

This figure introduces the Neural Network Fitting app, explaining its purpose, which is to solve an input-output fitting problem using a two-layer feed-forward neural network.

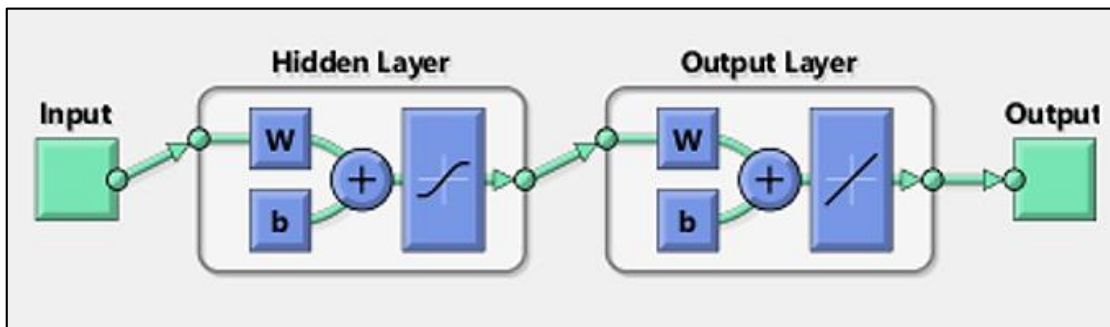


Figure (III.11):Neural Network Structure

The diagram shows the structure of the neural network, which includes an input layer, hidden layers, and an output layer.

Training Algorithm:It mentions that the network will be trained using the Levenberg-Marquardt back propagation algorithm (trainlm).

Inputs and Targets: This figure allows you to select the input and target data from the MATLAB workspace.

Data Summary: The summary on the right shows the dimensions of the selected data. Here, 'simplefitInputs' and 'simplefitTargets' are used as example datasets, with 94 samples each.

### 3. Import Data:

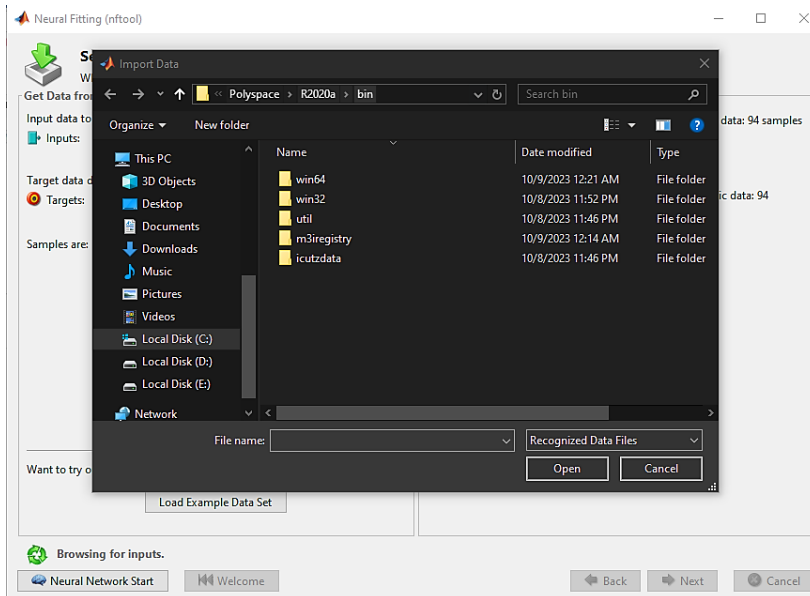


Figure (III.12): Import Data

Data Import: If the data is not already in the workspace, this figure allows you to browse and import data files from your computer. This ensures that the input and target datasets are correctly loaded into MATLAB for network training.

### 4. Validation and Test Data:

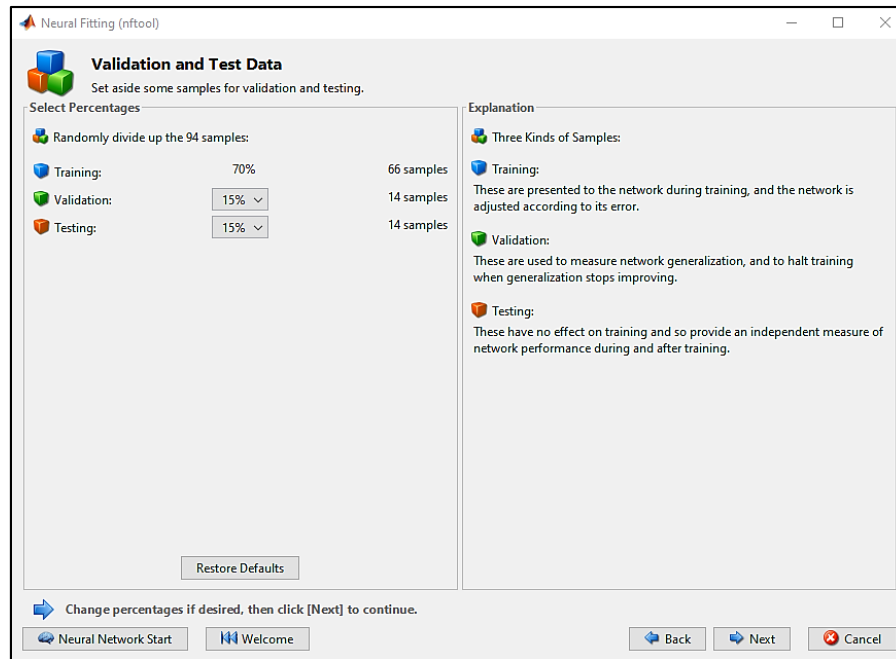


Figure (III.13): Validation and Test Data

**Data Division:** This figure divides the dataset into training, validation, and testing subsets. The default division is 70% training, 15% validation, and 15% testing.

**Explanation:** Training data is used to train the network, validation data is used to prevent overfitting by stopping training when performance worsens, and testing data is used to independently assess the network's performance.

## 5. Network Architecture:

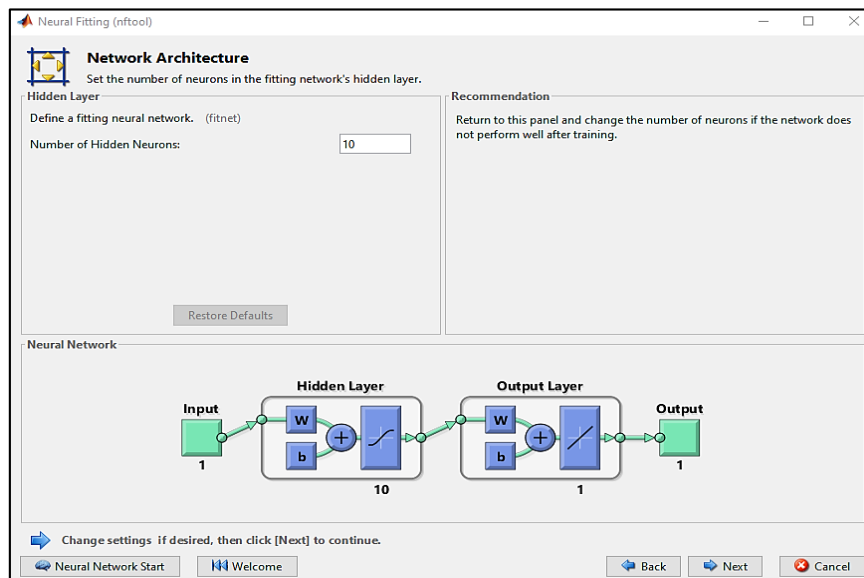
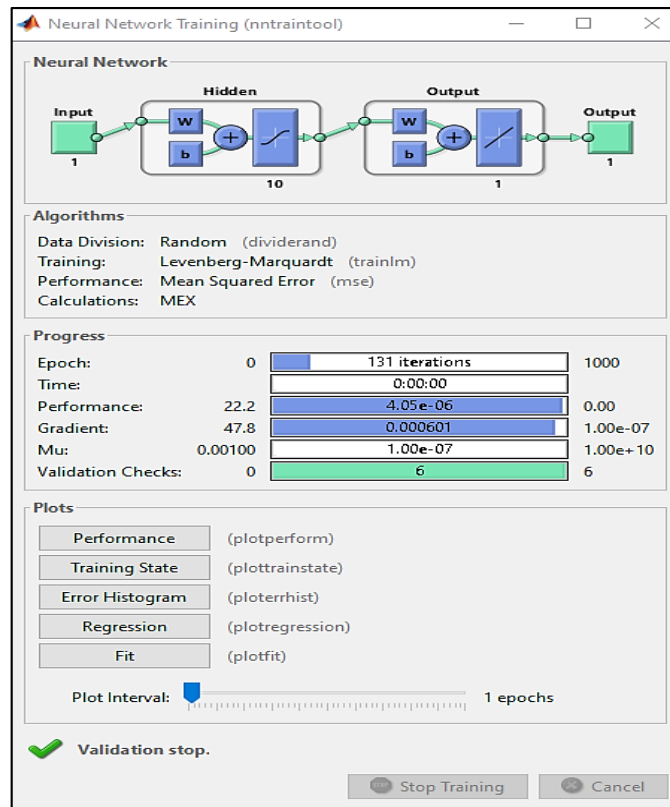


Figure (III.14): Network Architecture

Hidden Layer Configuration: This figure allows you to set the number of neurons in the hidden layer(s). In this example, there are 10 neurons in the hidden layer[36].

Network Diagram: The diagram below visually represents the structure of the network with the specified number of hidden neurons.

## 6. Network Training :



**Figure (III.15):**Network Training

Training Process: This figure shows the progress of the network training, including the number of epochs, performance, gradient, and validation checks.

Performance Plots: Various plots are available to monitor the training process, including performance, training state, error histogram, and regression plots.

Stop Training: You can manually stop the training process if needed[36]

### Train Network :

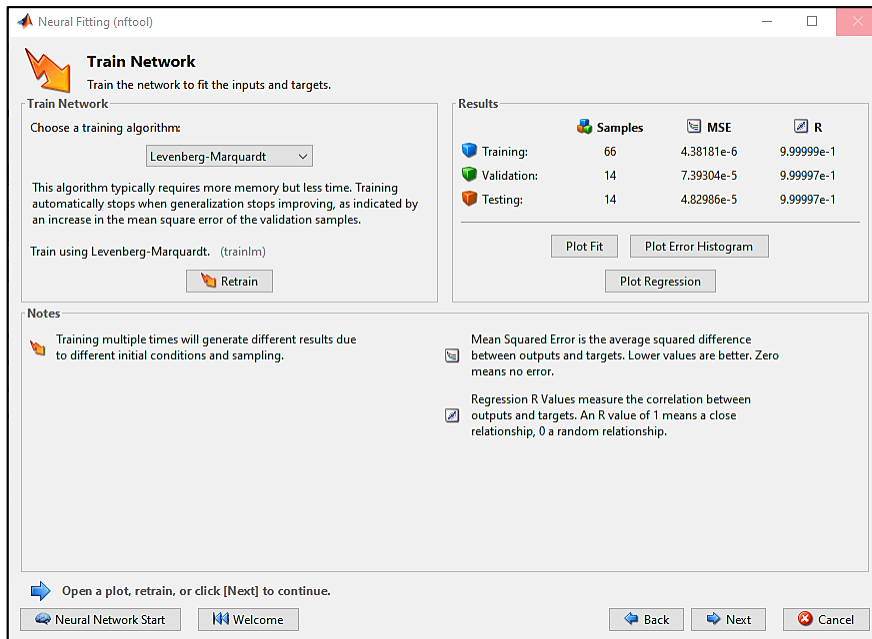


**Figure (III.16):**Train Network

Training Results: After training, this figure shows the results, including the mean squared error (MSE) for the training, validation, and testing datasets.

Regression Plot: This plot shows the correlation between the network outputs and the targets. A high R-value close to 1 indicates a good fit.

Error Histogram: This plot shows the distribution of errors between the network outputs and the targets[36].

### III.6. Conclusion :

This chapter introduces the most critical and complex aspect of the study. It focuses on the principle of maximum power point tracking (MPPT) and provides an overview of the various classifications of MPPT techniques. A detailed examination of the most commonly encountered MPPT methods in the literature has been presented. The diversity of MPPT techniques highlights the dynamic nature of this research area, emphasizing the challenges in identifying one or more universally applicable solutions.

# **Chapter IV**

## **Simulation Results**

### IV.1. Introduction:

This chapter presents a comprehensive performance evaluation and comparative analysis of three widely utilized Maximum Power Point Tracking (MPPT) algorithms: Perturb and Observe (P&O), Incremental Conductance (INC), and Artificial Neural Network (ANN). These algorithms are integral to enhancing the efficiency of photovoltaic (PV) systems by continuously adjusting the operating point to ensure optimal energy extraction from solar panels. Effective tracking of the maximum power point significantly contributes to the overall performance and energy yield of PV systems. The P&O algorithm operates by introducing periodic perturbations and monitoring the resulting changes to identify the optimal operating point. In contrast, the INC algorithm employs the incremental conductance approach to achieve more precise adjustments. The ANN-based algorithm utilizes artificial intelligence techniques to predict and track the maximum power point with a high degree of accuracy. This analysis aims to elucidate the respective advantages and limitations of each algorithm, thereby offering valuable insights into their applicability under varying operational conditions.

### IV.2. Parameters of System Simulation:

The following characteristics of panel and the parameters of boost converter that are used in our system simulation, are shown in the figure and table below:

Module data	
Module:	User-defined
Maximum Power (W)	200.22
Cells per module (Ncell)	60
Open circuit voltage Voc (V)	57.6
Short-circuit current Isc (A)	4.6
Voltage at maximum power point Vmp (V)	47
Current at maximum power point Imp (A)	4.26
Temperature coefficient of Voc (%/deg.C)	-0.35502
Temperature coefficient of Isc (%/deg.C)	0.06

**Figure (IV.1):** Characteristics of Panel

Boost Converter	Value
Capacitor 1	200 $\mu$ F
Inductor	3.5 mH
Capacitor 2	100 $\mu$ F
Resistive Load	300 $\Omega$

**Table (IV.1):** Parameters of Boost Converter

IV.3. Simulation Results:

IV.3.1. Constant Irradiance (1000 W/m<sup>2</sup>) :

a) P&O Algorithm :

In this simulation, we used the Perturb and Observe (P&O) algorithm to obtain results for power, voltage, and current. Figure (IV.2) represents the general system simulation, showcasing the overall setup and performance of the P&O -based MPPT system. The figure illustrates the integration of PV panels with the P&O -based MPPT controller, which adjusts the duty cycle to optimize power extraction.

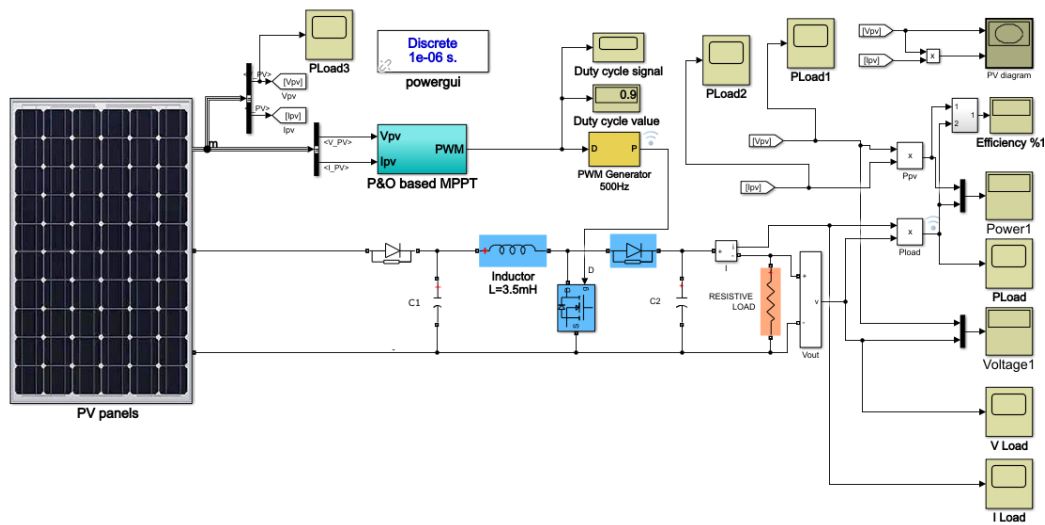


Figure (IV.2): Schema of System Simulation With P&O

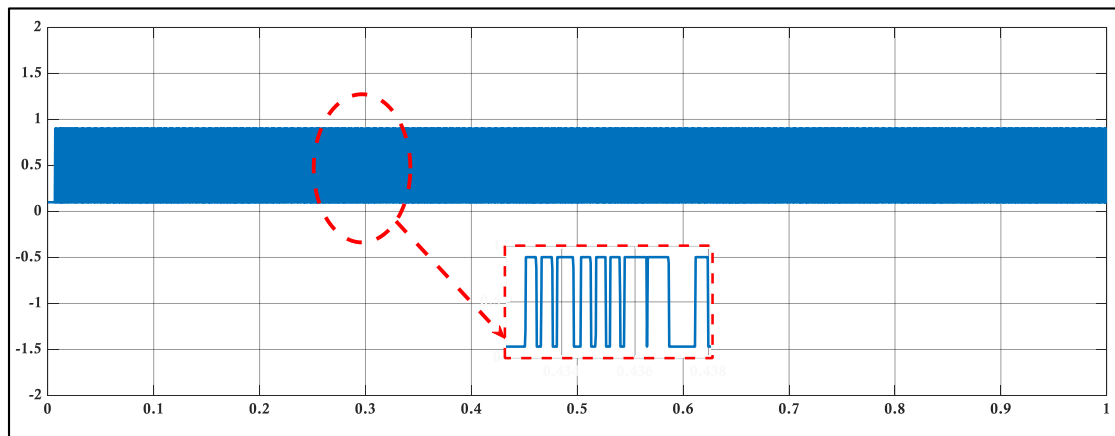
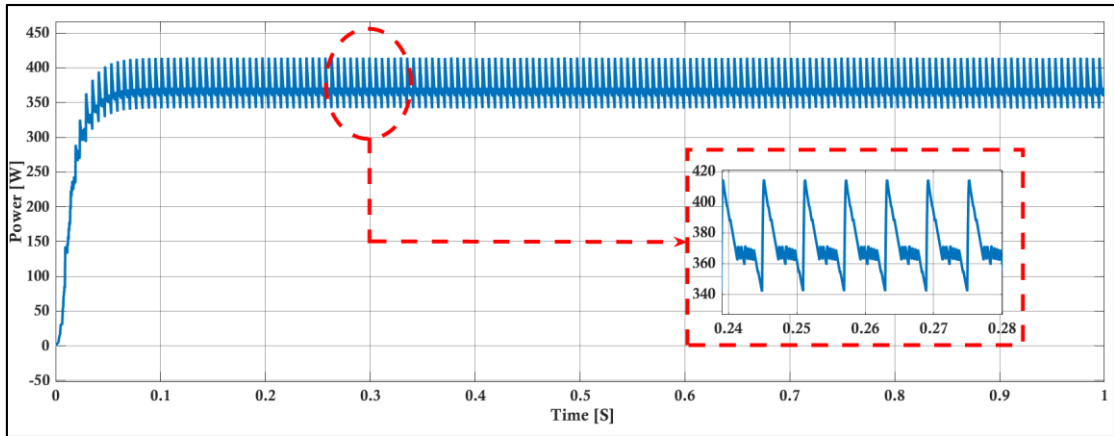


Figure (IV.3): Duty Cycle Simulation Result

The Figure (IV.3) demonstrates the MPPT system's duty cycle behavior, with the main plot showing overall stability and the zoomed-in view revealing critical fluctuations for precise MPPT operation.



**Figure (IV.4):** Power Simulation Result

The Figure (IV.4) illustrates the power response of an MPPT system using the P&O algorithm. The main plot shows a rapid increase in power followed by stabilization around 400W. The zoomed-in view highlights the oscillatory nature of the power output, characteristic of the P&O algorithm as it continuously perturbs to track the maximum power point. These oscillations are a trade-off for maintaining optimal power extraction and are crucial for understanding the efficiency and performance of the MPPT system.

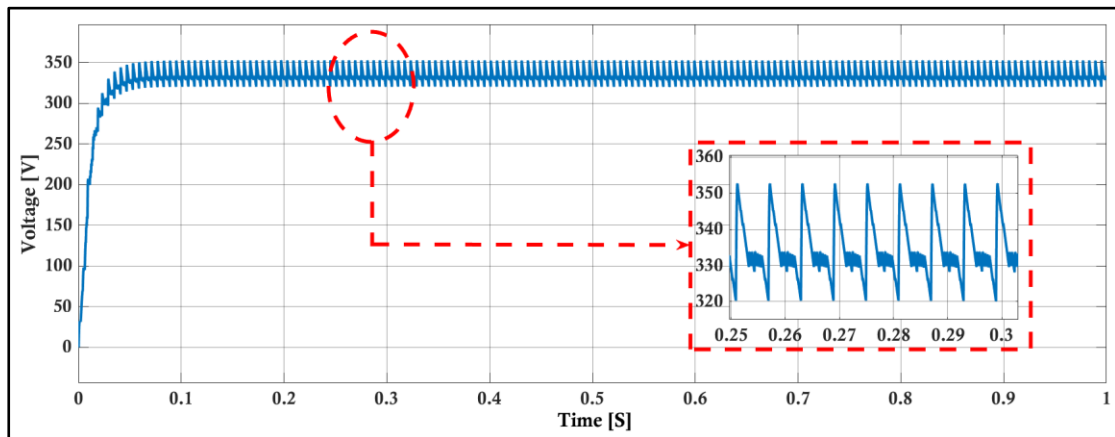


**Figure (IV.5):** Voltage Simulation Result

The Figure (IV.5) illustrates the voltage response of an MPPT system using the P&O algorithm. The main plot shows a rapid increase in voltage, stabilizing around 350V. The zoomed-in view highlights the oscillatory nature of the voltage output.

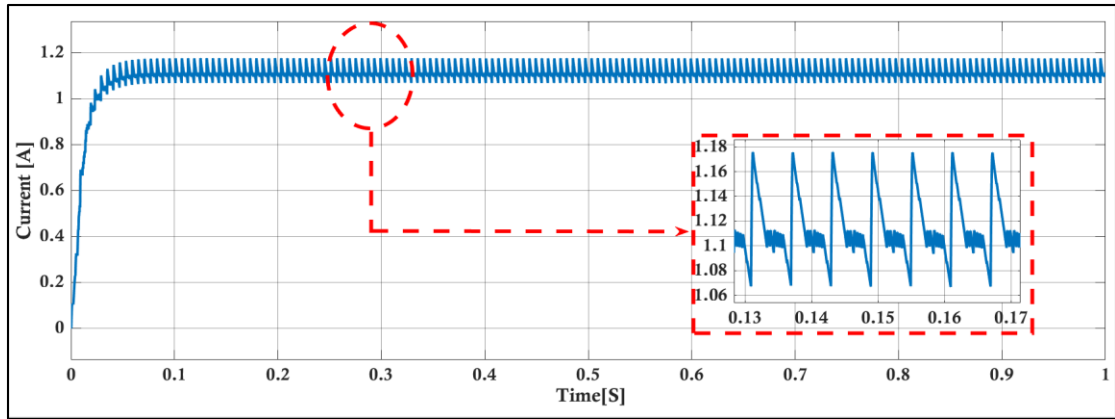


Figure (IV.6): Current Simulation Result

The Figure (IV.6) illustrates the current response of an MPPT system using the P&O algorithm. The main plot shows the rapid transient response leading to stabilization at approximately 1.12A, indicative of the system reaching its maximum power point. The zoomed-in view provides a closer look at the inherent oscillations around this steady-state value.

**b) Incremental Conductance:**

In this simulation, we used the Incremental Conductance (INC) algorithm to obtain results for power, voltage, and current. Figure (IV.7) represents the general system simulation, showcasing the overall setup and performance of the INC-based MPPT system. The figure illustrates the integration of PV panels with the INC-based MPPT controller, which adjusts the duty cycle to optimize power extraction.

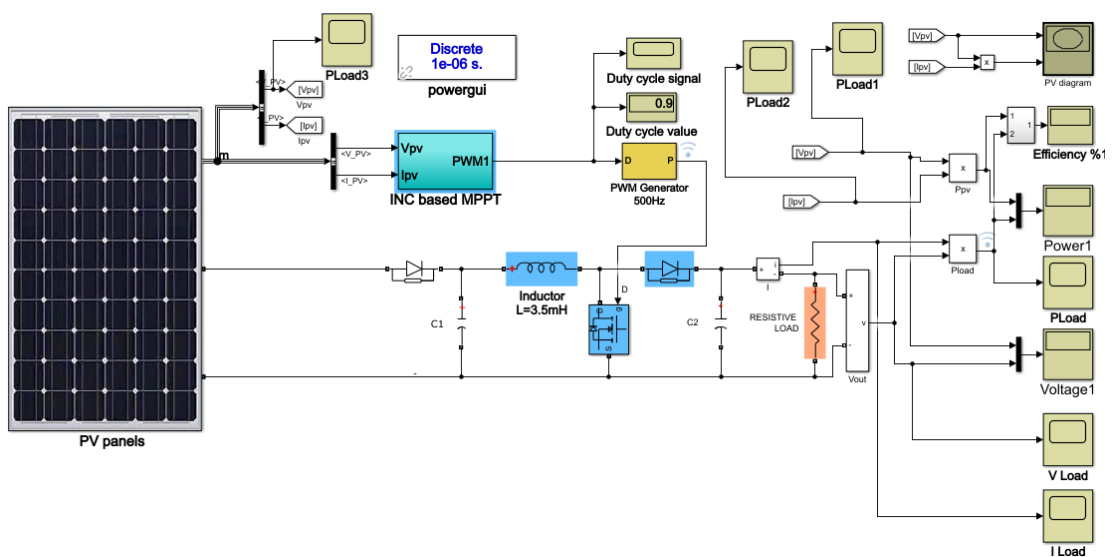
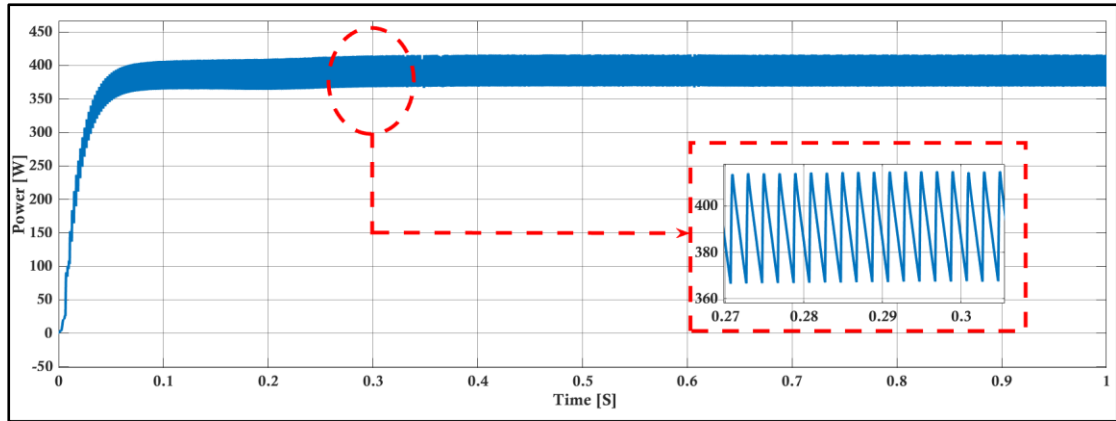
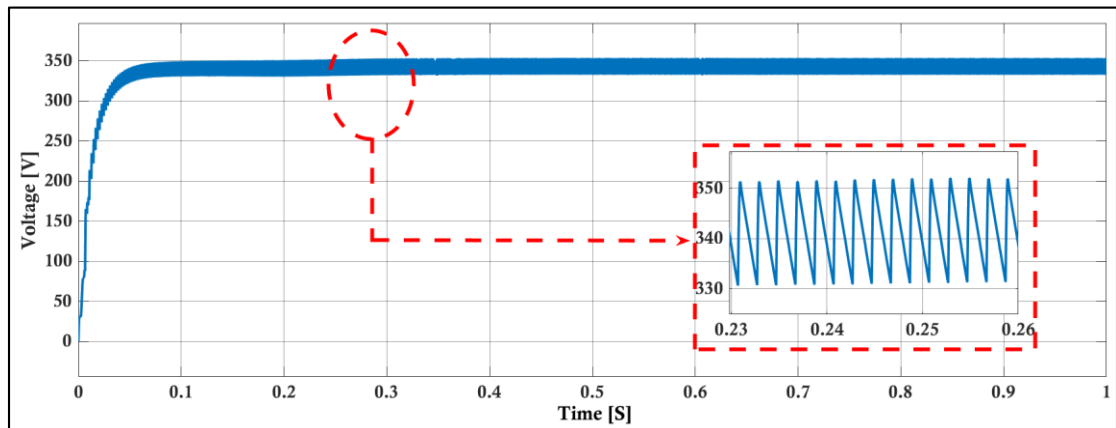


Figure (IV.7): Schema of System Simulation With INC



**Figure (IV.8):** Power Simulation Result

The Figure (IV.8) demonstrates the power stabilization behavior of an MPPT system managed by the Incremental Conductance algorithm. The main plot shows a rapid rise and stabilization of power at approximately 400W, reflecting the system's efficiency. The zoomed-in view highlights periodic fluctuations, illustrating the algorithm's continuous adjustments to maintain optimal power output. This analysis underscores the Incremental Conductance algorithm's capability to dynamically track the maximum power point with precision.



**Figure (IV.9):** Voltage Simulation Result

The Figure (IV.9) demonstrates the voltage response of an Incremental Conductance-based MPPT system. The main plot shows the voltage stabilizing around 345V, while the zoomed-in view captures small fluctuations.



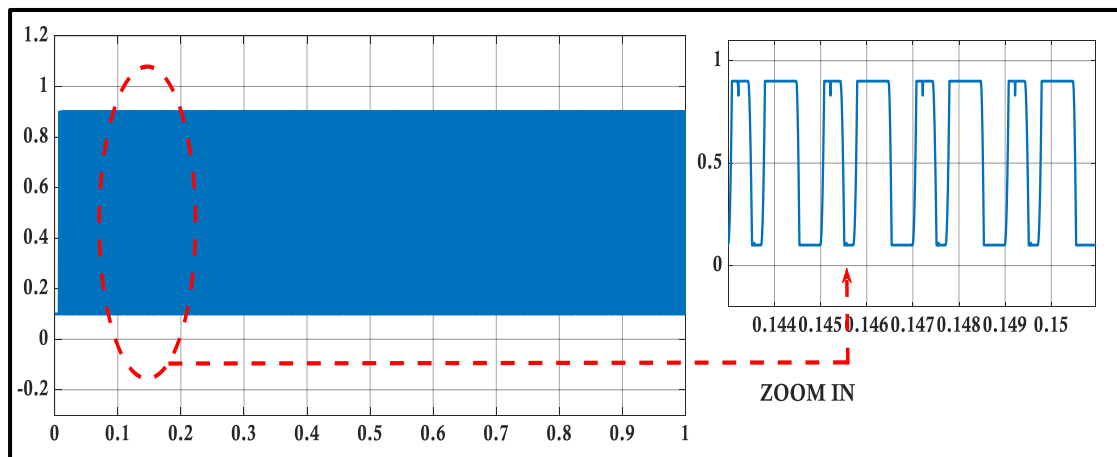


**Figure (IV.12):** Duty Cycle Simulation Result

The Figure (IV.12) demonstrates the stability and fine-tuning of the duty cycle by an ANN-based MPPT system. The main plot shows a stable duty cycle near 1, while the zoomed-in view reveals periodic adjustments, indicating the ANN's responsiveness to optimize performance.

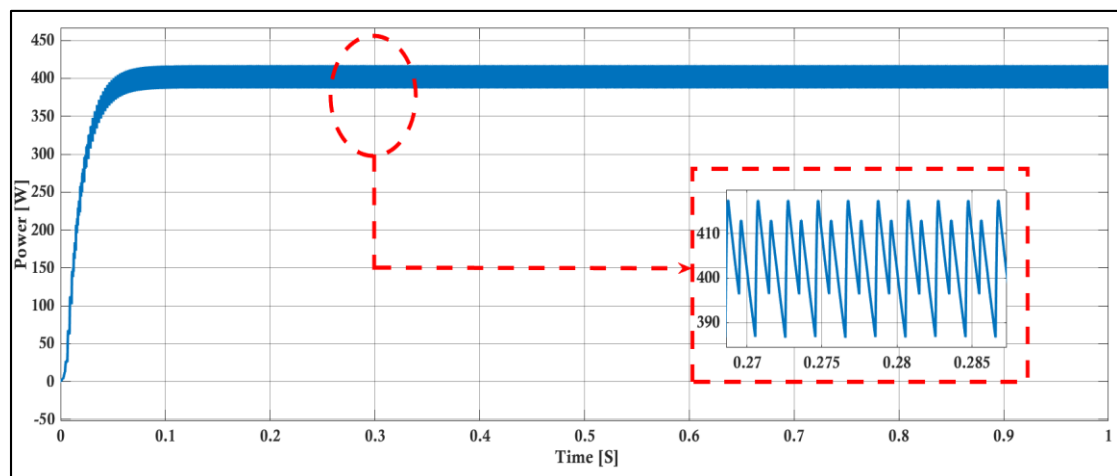


**Figure (IV.13):** Power Simulation Result

The Figure (IV.13) demonstrates the power stabilization behavior of an MPPT system managed by an ANN algorithm. The main plot indicates a rapid rise and stabilization of power at approximately 410W, reflecting the system's efficiency. The zoomed-in view highlights periodic fluctuations, illustrating the ANN's ongoing adjustments to maintain optimal power output. This analysis underscores the ANN algorithm's capability to dynamically track the maximum power point with precision.

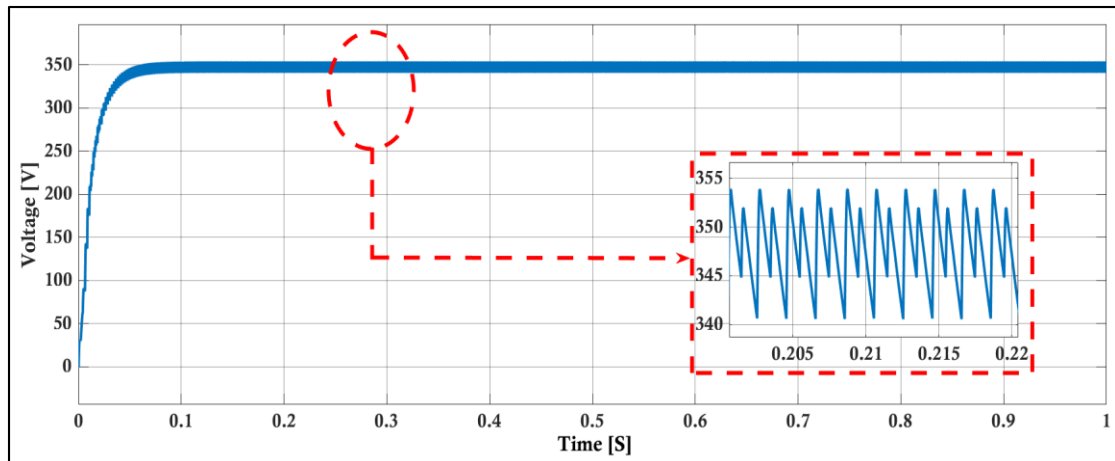


**Figure (IV.14):** Voltage Simulation Result

The Figure (IV.14) illustrates the voltage behavior of an ANN-based MPPT system. The main plot shows a quick rise and stabilization around 340V, while the zoomed-in view captures small fluctuations.

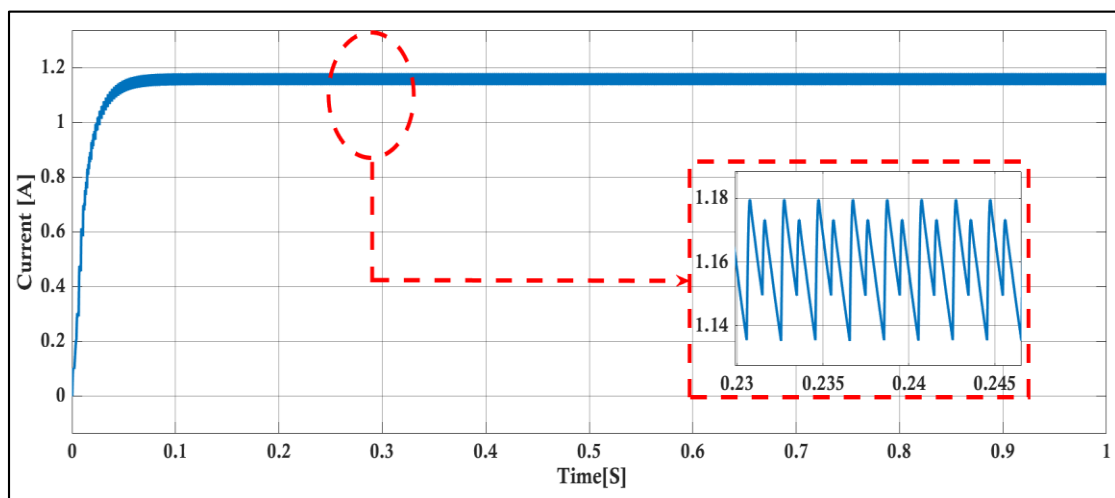


**Figure (IV.15):** Current Simulation Result

The Figure (IV.15) shows the current stabilization of an ANN-based MPPT system. The main plot displays a rapid rise in current, stabilizing around 1.16A. The zoomed-in view highlights small fluctuations.

### IV.3.2. Variable Irradiances (1000, 800, 600, 1000 W/m<sup>2</sup>):

#### a) P&O Algorithm :

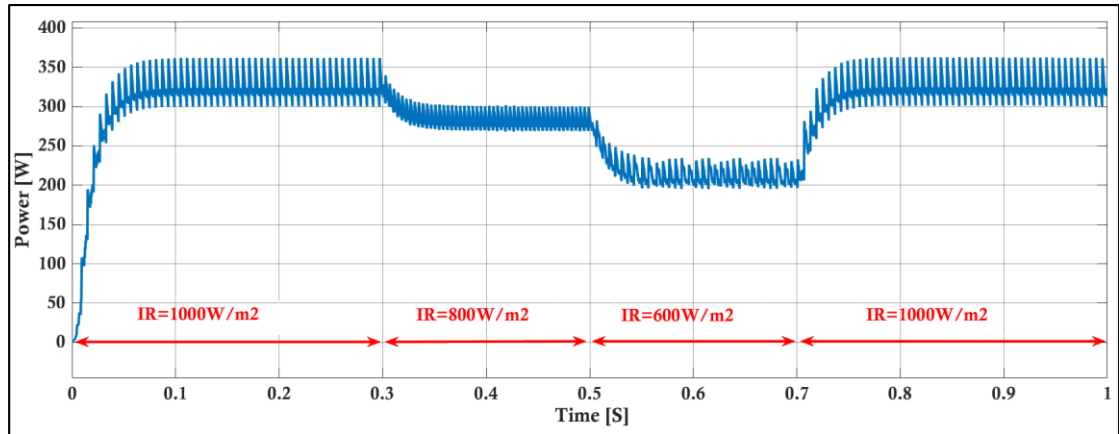
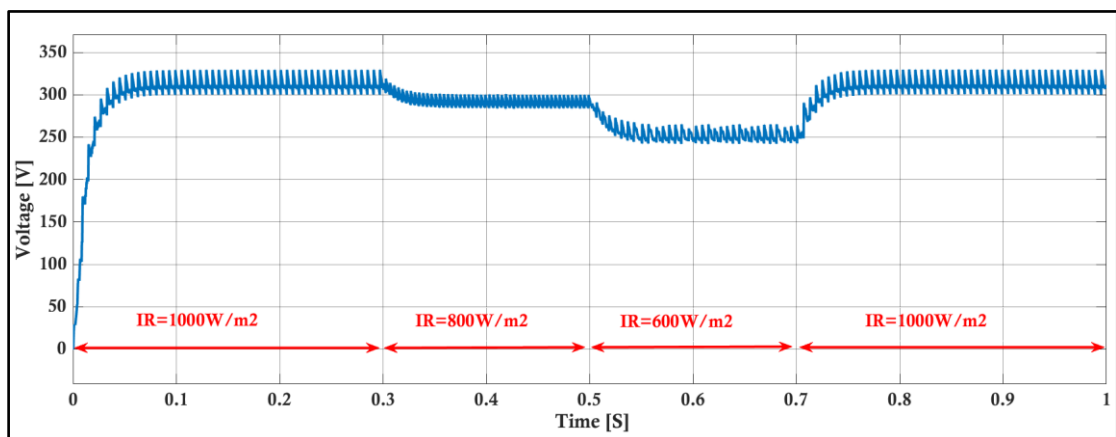


Figure (IV.16): Power Simulation Result

The Figure (IV.16) provides a comprehensive view of the MPPT system's power output behavior under varying irradiance levels. The main plot demonstrates the system's ability to track the maximum power point across different irradiances, with power stabilizing at approximately 350 W, 300W, 250W, and 370W for IR levels of 1000 W/m<sup>2</sup>, 800 W/m<sup>2</sup>, 600 W/m<sup>2</sup>, and 1000 W/m<sup>2</sup>, respectively. The red dashed ellipse and zoomed-in view emphasize the system's transient response to a sudden drop in irradiance, showcasing the characteristic oscillations as the P&O algorithm adjusts to the new maximum power point. This detailed analysis underscores the efficiency and adaptability of the MPPT system in real-time solar energy applications.



Figure(IV.17): Voltage Simulation Result

The Figure (IV.17) demonstrates how the voltage of an MPPT system using the P&O algorithm adjusts to varying irradiance levels. The main plot shows the system's quick

voltage stabilization at around 320V, followed by stepwise decreases as the irradiance drops. The zoomed-in view provides a detailed look at the transient fluctuations, illustrating the algorithm's continuous adjustments to maintain optimal performance.

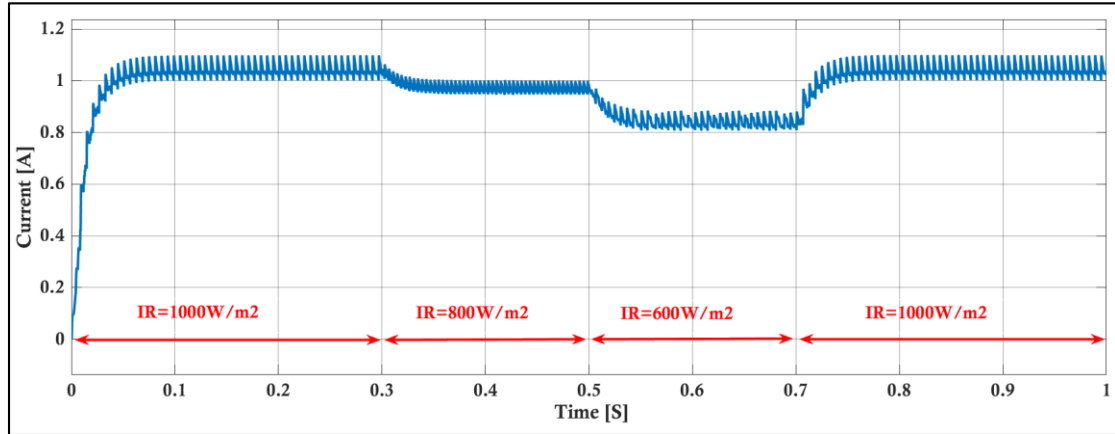


Figure (IV.18): Current Simulation Result

The Figure (IV.18) demonstrates how the MPPT system's current output, managed by the P&O algorithm, adjusts under varying irradiance levels. The main plot shows the current stabilizing around 1A and decreasing in steps as irradiance diminishes. The zoomed-in view captures the transient response during an irradiance change.

#### b) Incremental Conductance :

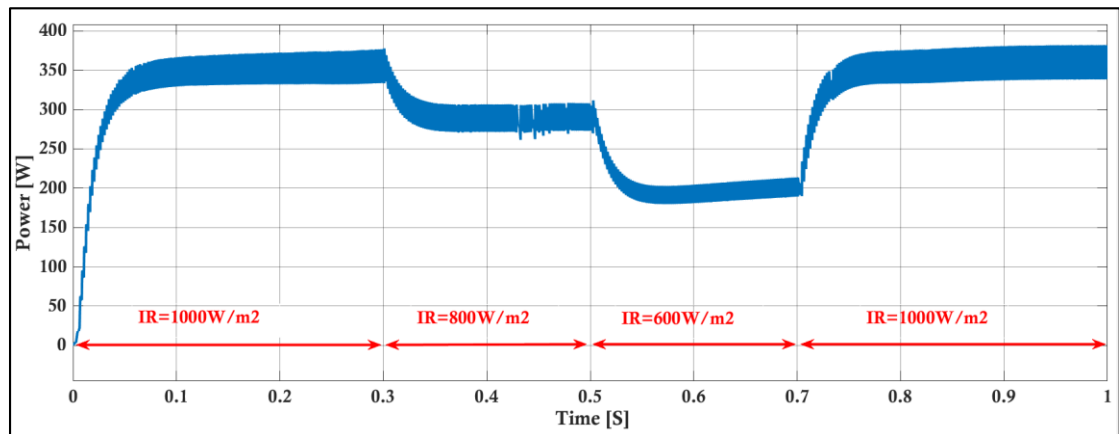
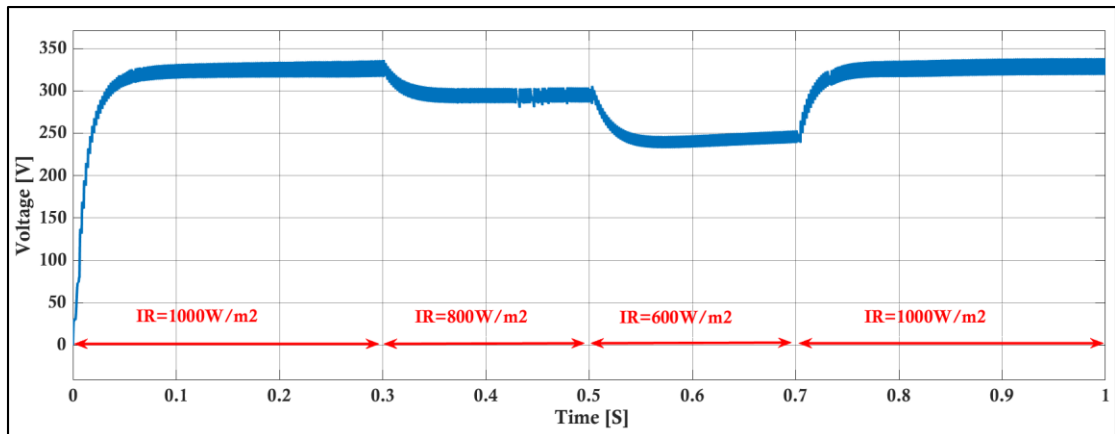


Figure (IV.19): Power Simulation Result

The Figure (IV.19) demonstrates the power response of an MPPT system using the Incremental Conductance algorithm under varying irradiance conditions. The main plot shows the power stabilizing around 350W initially, with stepwise decreases as the irradiance drops. The zoomed-in view captures the transient fluctuations during an irradiance change.



**Figure (IV.20):** Voltage Simulation Result

The Figure (IV.20) demonstrates the voltage response of an Incremental Conductance-based MPPT system to varying irradiance levels. The main plot shows a rapid rise and stabilization around 330V, with stepwise decreases as irradiance drops. The zoomed-in view highlights transient fluctuations,

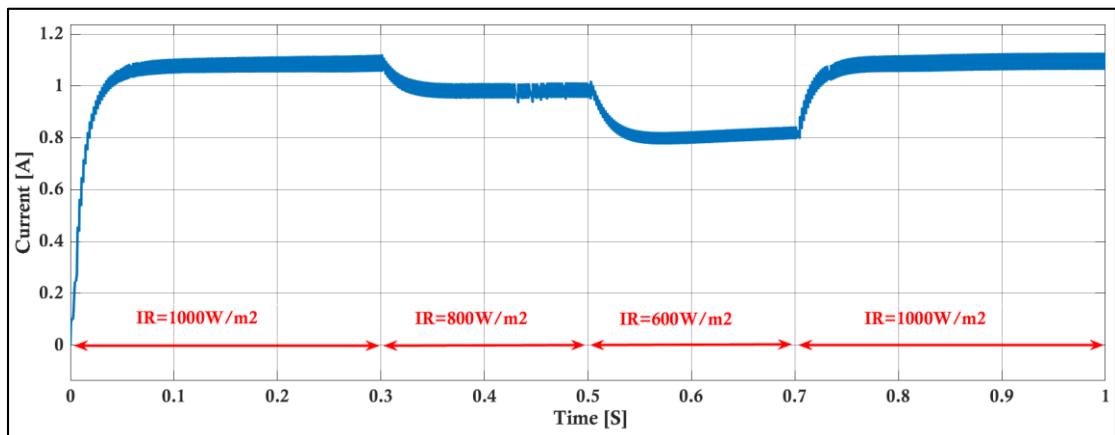


**Figure (IV.21):** Current Simulation Result

The Figure (IV.21) demonstrates the current response of an MPPT system using the Incremental Conductance algorithm under varying irradiance conditions. The main plot shows the current stabilizing around 1.1A initially, with stepwise decreases as the irradiance drops. The zoomed-in view captures transient fluctuations during an irradiance change.

## c) Artificial Neural Network (ANN):

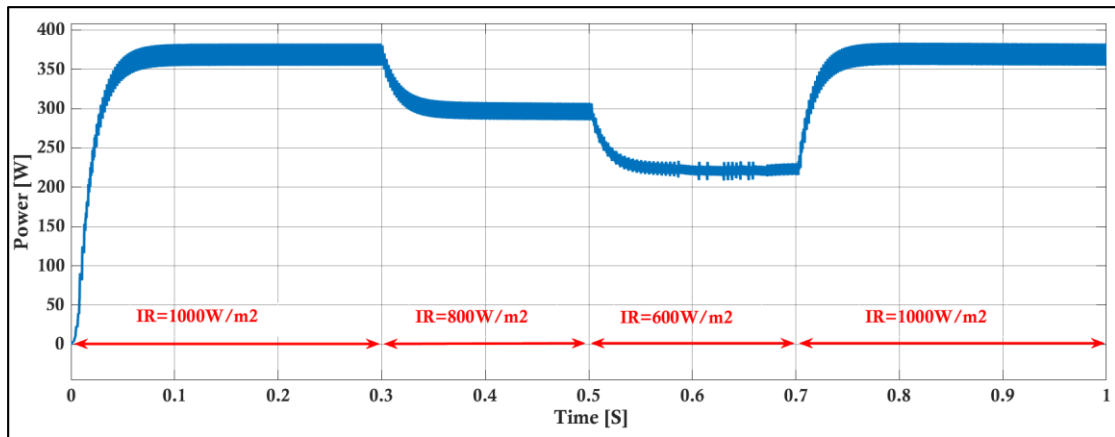


Figure (IV.22): Power Simulation Result

The Figure (IV.22) demonstrates how the ANN-based MPPT system adjusts its power output under varying irradiance conditions. The main plot shows the power stabilizing at approximately 350W initially, with stepwise decreases as the irradiance drops. The zoomed-in view captures the transient fluctuations during an irradiance change.

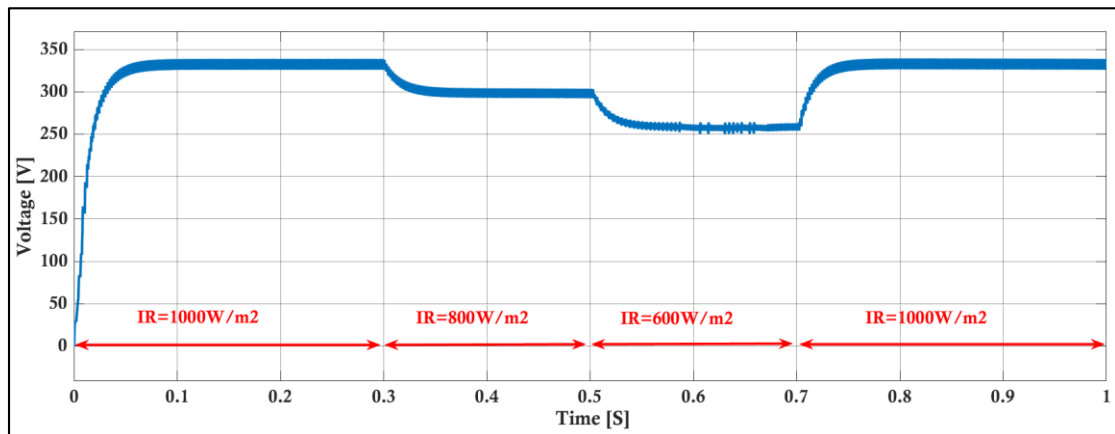


Figure (IV.23): Voltage Simulation Result

The Figure (IV.23) illustrates the ANN-based MPPT system's voltage response to varying irradiance. The main plot shows the voltage stabilizing around 330V and stepping down with decreasing irradiance. The zoomed-in view highlights transient fluctuations. This demonstrates the algorithm's capability to dynamically adjust to real-time changes in solar irradiance, ensuring efficient performance.

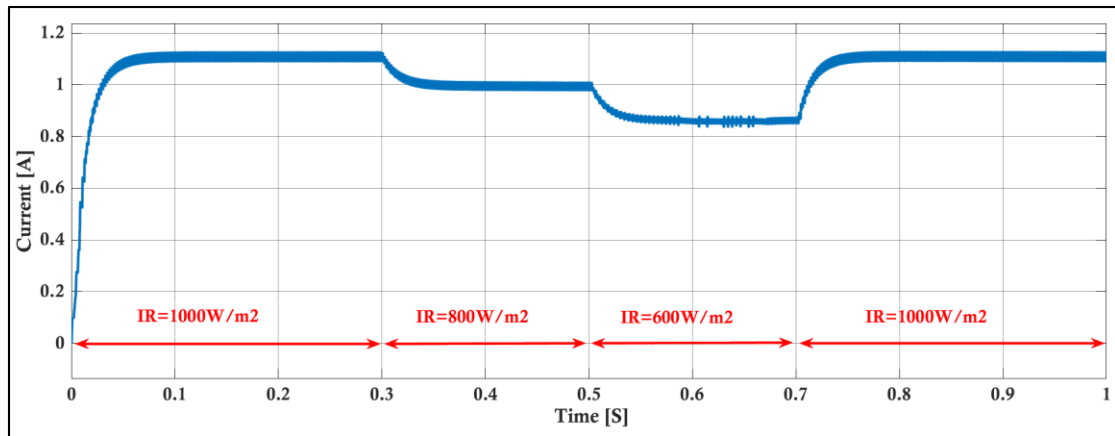


Figure (IV.24): Current Simulation Result

The Figure (IV.24) demonstrates the current response of an ANN-based MPPT system under varying irradiance conditions. The main plot shows the current stabilizing around 1.1A initially, with stepwise decreases as the irradiance drops. The zoomed-in view captures transient fluctuations during an irradiance change.

#### IV.4. Comparison of efficiency between algorithms (P&O, INC, ANN):

##### IV.4.1. Constant Irradiance(1000 W/m<sup>2</sup>):

Algorithm	Efficiency
Perturb and Observe (P&O)	95.2%
Incremental Conductance (INC)	96.06%
Artificial Neural Network (ANN)	97.11%

Table(IV.2): Table of Efficiency

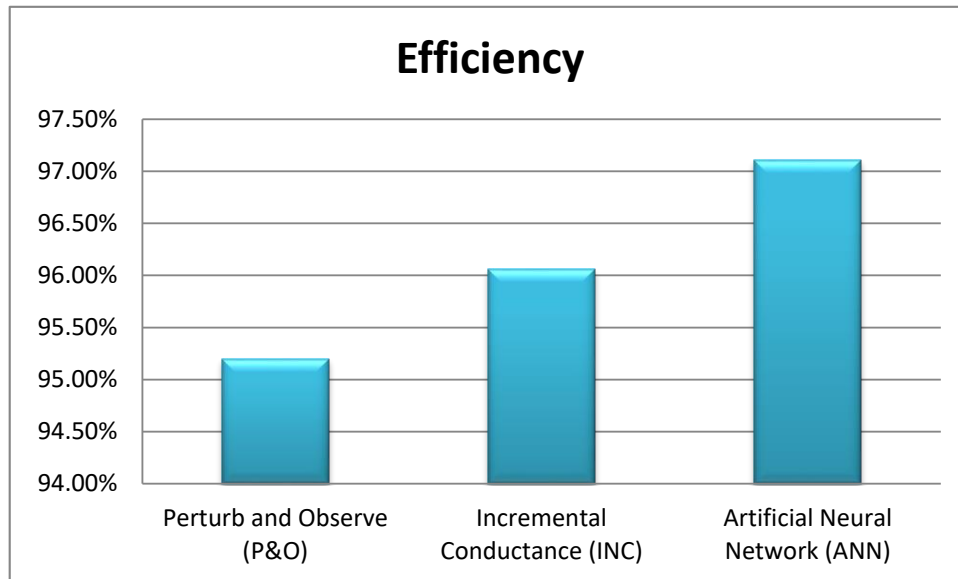


**Figure (IV.25):**Chart of Efficiency

Under constant irradiance of  $1000 \text{ W/m}^2$ , the Artificial Neural Network (ANN) algorithm demonstrates the highest efficiency, around 97%. The Incremental Conductance (INC) algorithm follows with an efficiency of about 96%, while the Perturb and Observe (P&O) algorithm has the lowest efficiency at approximately 95%. This indicates that the ANN algorithm is the most effective in optimizing power output under stable irradiance conditions, outperforming both the INC and P&O algorithms.

#### IV.4.2. Variable Irradiances (1000, 800, 600,1000W/m<sup>2</sup>):

Algorithm	Efficiency
Perturb and Observe (P&O)	85.32%
Incremental Conductance (INC)	88.52%
Artificial Neural Network (ANN)	95.54%

**Table(IV.3):** Table of Efficiency

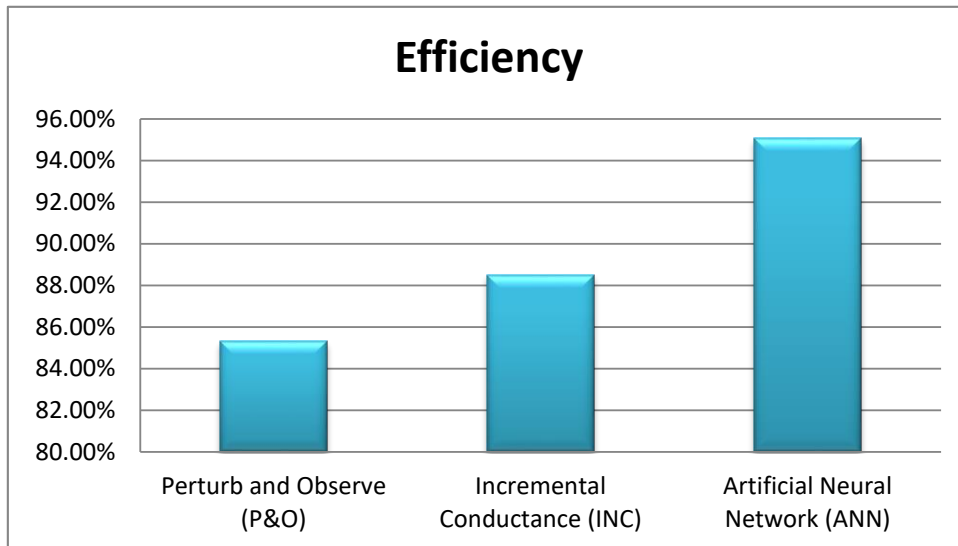


**Figure (IV.26):** Chart of Efficiency

Under variable irradiance conditions, the Artificial Neural Network (ANN) algorithm demonstrates the highest efficiency, around 95%, indicating its superior ability to adapt to changing light conditions. The Incremental Conductance (INC) algorithm follows with an efficiency of about 89%, showing reasonable performance but less stability compared to ANN. The Perturb and Observe (P&O) algorithm has the lowest efficiency at approximately 86%, reflecting its greater susceptibility to fluctuations under varying irradiance levels. These results highlight the ANN algorithm's effectiveness in optimizing power output in dynamic environments.

### **I.5. Conclusion:**

Among the evaluated Maximum Power Point Tracking (MPPT) methods, the Artificial Neural Network (ANN) algorithm emerges as the most effective and reliable. Its superior performance in terms of efficiency, stability, and adaptability under both steady-state and dynamically changing irradiance conditions positions it as the optimal choice for enhancing the output of photovoltaic (PV) systems. Although the Incremental Conductance (INC) algorithm demonstrates improved performance relative to the Perturb and Observe (P&O) method, it remains inferior to the advanced capabilities exhibited by the ANN approach. The P&O algorithm, despite its widespread application, is identified as the least effective among the three, characterized by lower efficiency and increased instability. Consequently, to maximize energy extraction and ensure consistent performance, the ANN algorithm is recommended as the preferred MPPT technique .

**General**

**Conclusion**

### General Conclusion

This study commenced by establishing a foundational understanding of solar radiation and the principles underlying photovoltaic (PV) energy conversion. It elucidated the mechanism by which solar cells utilize the photovoltaic effect to generate electrical energy from sunlight, and further examined the modeling, operational characteristics, and key factors influencing the efficiency of photovoltaic generators. Various types of PV cells, categorized according to their silicon crystal structures, were also presented. Subsequently, the study explored the essential role of DC-DC converters within power management systems. These converters enable efficient voltage regulation through distinct topologies, including buck, boost, and buck-boost configurations, thereby supporting their widespread application across numerous industrial domains. The concept of Maximum Power Point Tracking (MPPT) was then introduced as a critical technology in renewable energy systems, particularly in solar power applications. MPPT algorithms enhance energy harvesting by dynamically adjusting the electrical operating point to continuously align with the maximum power output of PV panels. This introduction naturally progressed to a comprehensive analysis of MPPT principles, classification schemes, and implementation techniques. Among the various MPPT algorithms assessed, the Artificial Neural Network (ANN) method was identified as the most effective and reliable. Its superior performance—characterized by high efficiency, stability, and adaptability under both steady-state and variable irradiance conditions—renders it the preferred approach for maximizing energy extraction and ensuring consistent system performance. Although other algorithms, such as Incremental Conductance (INC), demonstrated improved performance compared to the widely adopted Perturb and Observe (P&O) method, they were still outperformed by the advanced capabilities of the ANN-based approach. Accordingly, for optimal PV system output and long-term operational reliability, the ANN algorithm is determined to be the most suitable MPPT technique among those evaluated.

# References

- [1] Hohm, D. P., & Ropp, M. E. (2003). *Comparative study of maximum power point tracking algorithms*. *Progress in Photovoltaics: Research and Applications*, 11(1), 47–62.
- [2] Duffie, J. A., & Beckman, W. A. (2013). *Solar Engineering of Thermal Processes* (4th ed.). Wiley.
- [3] widell, J., & Weir, T. (2015). *Renewable Energy Resources* (3rd ed.). Routledge. Discusses various types of renewable energy, including solar radiation, the photovoltaic effect, and factors affecting solar panel performance.
- [4] Serway, R. A., & Jewett, J. W. (2014). *Physics for Scientists and Engineers* (9th ed.). Cengage Learning. Covers the full range of the electromagnetic spectrum and explains the inverse relationship between wavelength and energy
- [5] Messenger, R. A., & Ventre, J. (2010). *Photovoltaic Systems Engineering* (3rd ed.). CRC Press.
- [6] Luque, A., & Hegedus, S. (Eds.). (2011). *Handbook of Photovoltaic Science and Engineering* (2nd ed.). Wiley.
- [7] ESRAM, T., & CHAPMAN, P. L. (2007). Comparison of Photovoltaic Array Maximum Power Point Tracking Techniques. *IEEE Transactions on Energy Conversion*, 22(2), 439–449. <https://doi.org/10.1109/TEC.2006.874230>.
- [8] Green, M. A. (1982). *Solar Cells: Operating Principles, Technology, and System Applications*. Prentice-Hall.
- [9] Villalva, M. G., Gazoli, J. R., & Filho, E. R. (2009). Comprehensive Approach to Modeling and Simulation of Photovoltaic Arrays. *IEEE Transactions on Power Electronics*, 24(5), 1198–1208.
- [10] Sze, S. M. (1981). *Physics of Semiconductor Devices* (2nd ed.). Wiley-Interscience.
- [11] Masters, G. M. (2013). *Renewable and Efficient Electric Power Systems* (2nd ed.). Hoboken, NJ: Wiley

## References

---

- [12] EnergySage. (n.d.). Monocrystalline vs. polycrystalline solar panels. EnergySage. Retrieved from <https://www.energysage.com/solar/solar-panels/monocrystalline-vs-polycrystalline/>
- [13] Cotal, H., Fetzer, C., Boisvert, J., Kinsey, G., King, R., Hebert, P., Yoon, H., & Karam, N. (2009). III–V multijunction solar cells for concentrating photovoltaics. *Energy & Environmental Science*, 2(2), 174–192
- [14] Lorenzo, E. (1994). *Solar Electricity: Engineering of Photovoltaic Systems*. Progensa.
- [15] U.S. Department of Energy. (n.d.). Solar energy basics. Office of Energy Efficiency & Renewable Energy.
- [16] Texas Instruments. (n.d.). *Switching regulator fundamentals (Rev.C)*.
- [17] Erickson, R. W., & Maksimović, D. (2001). *Fundamentals of Power Electronics* (2nd ed.). Springer.
- [18] F. L. Luo and H. Ye, *Advanced dc/dc converters*. crc Press, 2016.
- [19] A. S. Y. Alzahrani, *Advanced topologies of high-voltage-gain DC-DC boost converters for renewable energy applications*. Missouri University of Science and Technology, 2018.
- [20] R. P. Severns, G. Bloom, and R. P. Severns, *Modern DC-to-DC switchmode power converter circuits*. Springer, 1985.
- [21] S. Chakraborty, H.-N. Vu, M. M. Hasan, D.-D. Tran, M. E. Baghdadi, and O. Hegazy, "DC-DC converter topologies for electric vehicles, plug-in hybrid electric vehicles and fast charging stations: State of the art and future trends," *Energies*, vol. 12, no. 8, p. 1569, 2019.
- [22] [https://www.toolify.ai/ai-news/complete-tutorial-implementing-ann-in-matlab-simulink-1764419#google\\_vignette](https://www.toolify.ai/ai-news/complete-tutorial-implementing-ann-in-matlab-simulink-1764419#google_vignette) (accessed).
- [23] M. D. S. M. C. Mr MEKKAOUI Saddam and AhmedYahia, "(Conception, simulation et réalisation d'un régulateur solaire avec commande MPPT à base d'une carte Arduino)", UNIVERSITE EchahidHamma Lakhdar- EL Oued, 2022.
- [24] M. K. B. Abdelheq, "ETUDE ET REALISATION D'UN CONVERTISSEUR DC-DC," Université Aboubakr BelkaÛd-Tlemcen, 2018.
- [25] S. ABOUDA, "« Contribution à la commande des systèmes photovoltaïques », " Université de Reims Champagne-Ardenne et université de Sfax, 2015.

## References

---

- [26] R. Touahir and M. B. Zahia, "contrôleur neuronal pour la poursuite du point de puissance maximale d'un système photovoltaïque," *Mémoire master, Université Kasdi Merbah, Ouargla, Algérie*, 2015.
- [27] S. H. E. Babaa, "High efficient interleaved boost converter with novel switch adaptive control in photovoltaic application," Newcastle University, 2013.
- [28] A. b. T. Bekhti Mohammed, "Maximum Power Point Tracking Simulations for PV Applications Using Matlab Simulink," *International Journal of Engineering Practical Research*, January 2014.
- [29] A. C. Pastor, "Conception et réalisation de modules photovoltaïques électroniques," INSA de Toulouse, 2006.
- [30] M. R. Patel, *Wind and solar power system*. CRC press, 1999.
- [31] R. Boukenoui, M. Ghanes, J.-P. Barbot, R. Bradai, A. Mellit, and H. Salhi, "Experimental assessment of Maximum Power Point Tracking methods for photovoltaic systems," *Energy*, vol. 132, pp. 324-340, 2017.
- [32] B. N. Alajmi, K. H. Ahmed, S. J. Finney, and B. W. Williams, "Fuzzy-logic-control approach of a modified hill-climbing method for maximum power point in microgrid standalone photovoltaic system," *IEEE transactions on power electronics*, vol. 26, no. 4, pp. 1022-1030, 2010.
- [33] A. A. Ghassami, S. M. Sadeghzadeh, and A. Soleimani, "A high performance maximum power point tracker for PV systems," *International Journal of Electrical Power & Energy Systems*, vol. 53, pp. 237-243, 2013.
- [34] G. Abdelmounaim, "An Advanced Neural Network-Based MPPT Controller for Photovoltaic Systems," University of El-Oued, 2023.
- [35] [https://www.toolify.ai/ai-news/complete-tutorial-implementing-ann-in-matlab-simulink-1764419#google\\_vignette](https://www.toolify.ai/ai-news/complete-tutorial-implementing-ann-in-matlab-simulink-1764419#google_vignette). (accessed).
- [36] <https://www.mathworks.com/help/deeplearning/ug/workflow-for-neural-network-design.html>. (accessed).